AD-A121 725 FEASIBILITY STUDY ON CNC MULTIOPERATION GRINDING OF JET 1/1
ENGINE COMPONENTS.(U) HAHN ASSOCIATES NORTHBOROUGH MA
R S HAHN 30 SEP 82 AFOSR-TR-82-0992 F49620-82-C-0056

UNCLASSIFIED F/G 13/8 NL

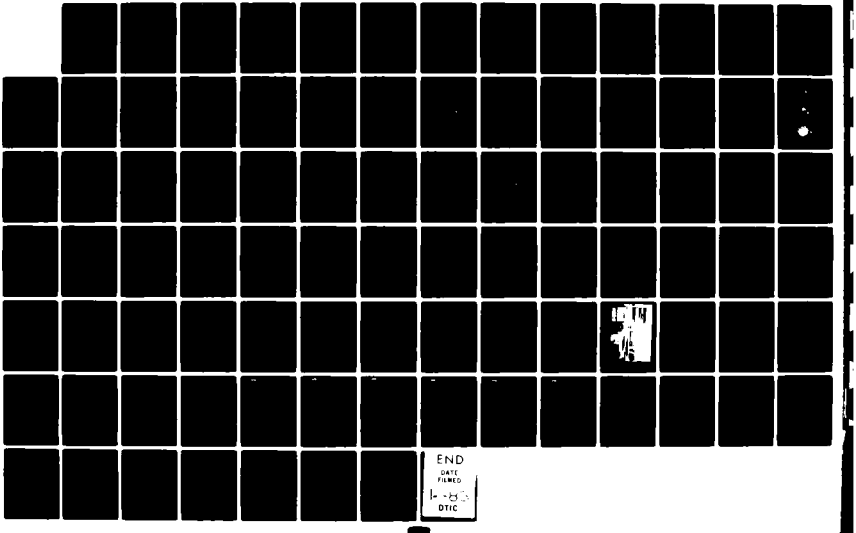

END
DATE FILMED
DTIC

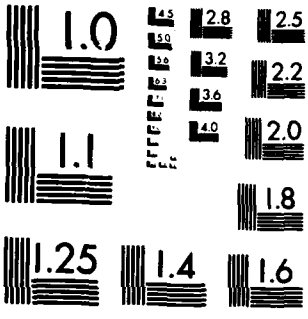

MICROCOPY RESOLUTION TEST CHART
NATIONAL BUREAU OF STANDARDS-1963-A

AFOSR-TR- 82-0992

Report F49620-82-C-0066

FEASIBILITY STUDY ON CNC MULTIOPERATION GRINDING OF JET ENGINE COMPONENTS USING FORCE SENSING ADAPTIVE CONTROL

Robert S. Hahn
Hahn Associates
26 Rice Avenue
Northboro, MA 01532

30 September 1982

Final Report for Period
1 April 1982 through 30 September 1982

Prepared for

USAF, AFSC
AIR FORCE OFFICE OF SCIENTIFIC RESEARCH
Building 410
Bolling AFB, D.C. 20332

Administered by

DCASMA BOSTON
495 Summer Street
Boston, MA 02210

SECURITY CLASSIFICATION UNCLASSIFIED (When Data Entered)

REPORT DOCUMENTATION PAGE	READ INSTRUCTIONS BEFORE COMPLETING FORM
1. REPORT NUMBER AFOSR-TR- 82-0992 ~~F49620-82-C-0066~~ 2. GOVT ACCESSION NO. AD-A	3. RECIPIENT'S CATALOG NUMBER
4. TITLE (and Subtitle) FEASIBILITY STUDY ON CNC MULTIOPERATION GRINDING OF JET ENGINE COMPONENTS USING FORSE-SENSING ADAPTIVE CONTROL.	5. TYPE OF REPORT & PERIOD COVERED Final Report for 1 APR'82 - 30 SEPT.'82
	6. PERFORMING ORG. REPORT NUMBER
7. AUTHOR(s) ROBERT S. HAHN	8. CONTRACT OR GRANT NUMBER(s) F49620-82-C-0066
9. PERFORMING ORGANIZATION NAME AND ADDRESS HAHN ASSOCIATES 26 RICE AVENUE NORTHBORO, MA 01532	10. PROGRAM ELEMENT, PROJECT, TASK AREA & WORK UNIT NUMBERS 61102F 2305/K1
11. CONTROLLING OFFICE NAME AND ADDRESS USAF - AFSC AIR FORCE OFFICE OF SCIENTIFIC RESEARCH BUILDING 410 BOLLING AFB, D.C. 20332	12. REPORT DATE 30 SEPT. '82
	13. NUMBER OF PAGES
14. MONITORING AGENCY NAME & ADDRESS(if different from Controlling Office) ~~DCASMA - BOSTON 495 SUMMER ST. BOSTON, MA 02210~~	15. SECURITY CLASS. (of this report) Unclassified
	15a. DECLASSIFICATION/DOWNGRADING SCHEDULE

16. DISTRIBUTION STATEMENT (of this Report)

Approved for Public Release--Distribution Unlimited

17. DISTRIBUTION STATEMENT (of the abstract entered in Block 20, if different from Report)

18. SUPPLEMENTARY NOTES

19. KEY WORDS (Continue on reverse side if necessary and identify by block number)

CNC GRINDING
ADAPTIVE CONTROL GRINDING
CREEP FEED GRINDING
COMPUTER-AIDED MANUFACTURE
MULTIOPERATION GRINDING
GRINDING JET ENGINE COMPONENTS

20. ABSTRACT (Continue on reverse side if necessary and identify by block number) This report describes methods for reducing costs in grinding jet engine components using computer control with grinding force sensors to obtain improved grinding performance. Multioperation grinding using two wheelheads on the same cross slide as well as on separate slides is discussed. A method for eliminating thermal size errors is presented. Formulas are given for estimating grinding cycles, stock-removal rates & wheelwear rates for both normal workspeed grinding and creep feed grinding. The computer, with the force sensors, can monitor(over)

DD FORM 1 JAN 73 1473 EDITION OF 1 NOV 65 IS OBSOLETE

UNCLASSIFIED
SECURITY CLASSIFICATION OF THIS PAGE (When Data Entered)

cont. block 20:

differential wheelwear and thereby prevent form errors. Wheel sharpness can also be monitored to avoid thermal damage.

PREFACE

The material in this report was derived, partly, by plant visitations. The cooperation of the following plants is greatly appreciated:

Pratt & Whitney Aircraft
North Haven, CT

Pratt & Whitney Aircraft
North Berwick, ME

General Electric Co.
Rutland, VT

Detroit Diesel-Allison Div. GMC
Indianapolis, Indiana

Cone Blanchard-Div. of Oerlikon
Windsor, VT

TABLE OF CONTENTS

TABLE OF CONTENTS--contd

NOMENCLATURE

V_w = Work surface speed (m/s)

N_w = Work speed (RPM)

V_s = Wheel surface speed (m/sec)

N_s = Wheel speed (RPM)

V_t = Traverse speed (m/sec)

D_w = Work diameter (mm)

D_s = Wheel diameter (mm)

ℓ = Dress lead (um/rev)

c = 2*diamond depth-of-dress (um)

d = Grain diameter (um)

D_e = Equivalent diameter (cm)

vol = 1.33H + 2.2S -8 (vol % of bond in wheel)

H = 0,1,2,3--- for H,I,J,K---hardness

S = wheel structure no.

F'_n = Normal force intensity (N/mm)

F_n = Normal force (N)

F_t = Tangential force (N)

F'_{th} = F'_{no} = Threshold force intensity (N/mm)

F'_{pc} = Plowing-cutting transition force intensity (N/mm)

F'_{bd} = Wheel breakdown force intensity (N/mm)

h = Wheel depth-of-cut (um)

α = Dimensionless machining--Elasticity number

P = Grinding Power (watts)

P_s = Specific Power (joules/cu.mm)

τ_o = Time Constant

l_c = Wheelwork Contact Length

R_c = Rockwell Hardness C Scale

NOMENCLATURE--contd.

WRP = Λ_w = Work Removal Parameter (cu.mm/min*N)

K_m = System Stiffness (N/um)

W = Width of Wheelwork Contact (mm)

$\bar{v}_f$ = Feedrate (um/sec)

$\bar{v}_w$ = Penetration velocity of wheel into work (um/sec)

$\bar{v}_s$ = Radial wheelwear velocity (um/sec)

Z_w = Volumetric rate of stock removal (cu.mm/sec)

Z'_w = Stock removal rate per unit width (sq.mm/sec)

Z_s = Volumetric wheelwear rate (cu.mm/sec)

Z'_s = Wheelwear rate per unit width (sq.mm/sec)

S = Wheel Sharpness (sq.m/N)

WWP = Wheelwear Parameter ($mm^4/min*N^2$)

K_c = $\frac{V_w w}{\Lambda_w}$ = "Cutting Stiffness" of workpiece (N/mm)

Δ = Difference in Curvature

P = Average Normal Pressure or Stress

WP = Wheelwear Parameter referred to Pressure

1.0 OBJECTIVES

The purpose of this work was to investigate potential cost savings in the manufacture of certain jet engine components that could be achieved through the use of computer-controlled, multi-operation grinding using force-sensing adaptive control systems.

Another objective was to provide a control system that would monitor and control the important grinding process variables so as to permit grinding machines to operate with little or no operator attention.

A third objective was to provide automatic size control, as well as form or contour control, that would not require constant attention from the operator.

A fourth objective was to evaluate "creep-feed" grinding in comparison to normal grinding with regard to stock removal, wheelwear,cycle time, and induced forces and deflections.

A fifth objective was to determine the rigidity requirements placed upon a machine by size and form tolerance specifications.

A further objective was to determine, under operating speeds, the force levels that could be detected and fed to a computer from a typical force sensor installed in a wheelhead.

2.0 MULTIOPERATION GRINDING--TWO WHEELHEADS--SINGLE CROSS SLIDE

Many workpieces produced in industry require several grinding operations. In batch-type manufacturing, significant savings can sometimes be achieved by performing a number of grinding operations for one setup or staging of the part. Two wheelheads mounted on a single cross slide often provide the versatility required to accomplish a set of grinding operations as illustrated in Fig. 1 where the computer can control the X and Z slide positions. The wheelheads can also be equipped with force transducers mounted inside the wheelhead and arranged to measure the grinding force thereby giving the computer the ability to control the grinding process variables and improve grinding performance. Force-sensing adaptive control will be described in Section 6.

The turbine vane segment shown in Fig. 2 illustrates a cost-effective, multioperation grinding application.

The current processing of this part requires five setups, eight operations and involves four machine tools as shown in the right-hand column of Table 1. One loading of the fixture produces 26 vane segments. The current total machining time is 9.37 hours, and does not include setup time for the five setups.

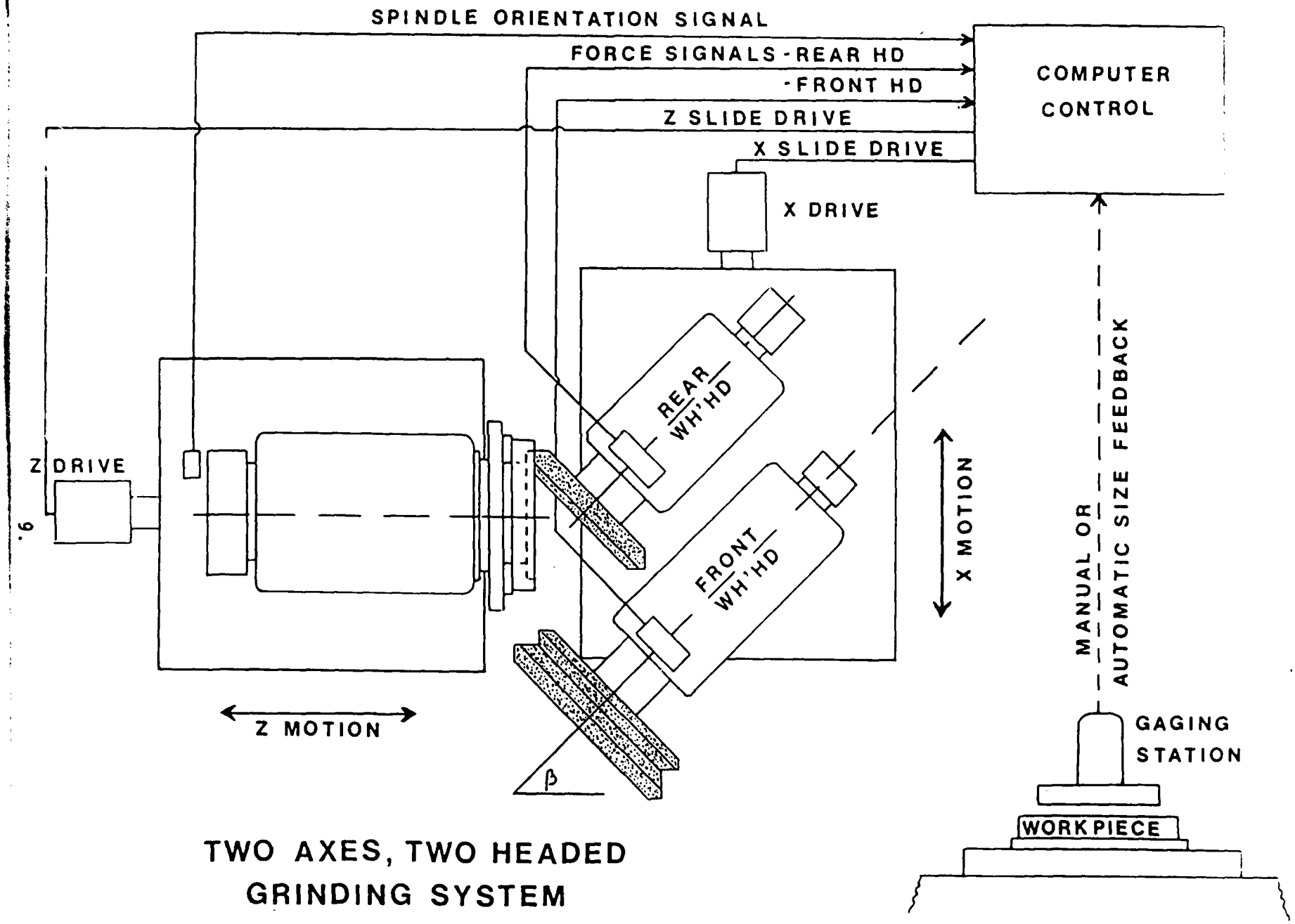

TWO AXES, TWO HEADED GRINDING SYSTEM

FIG. 1

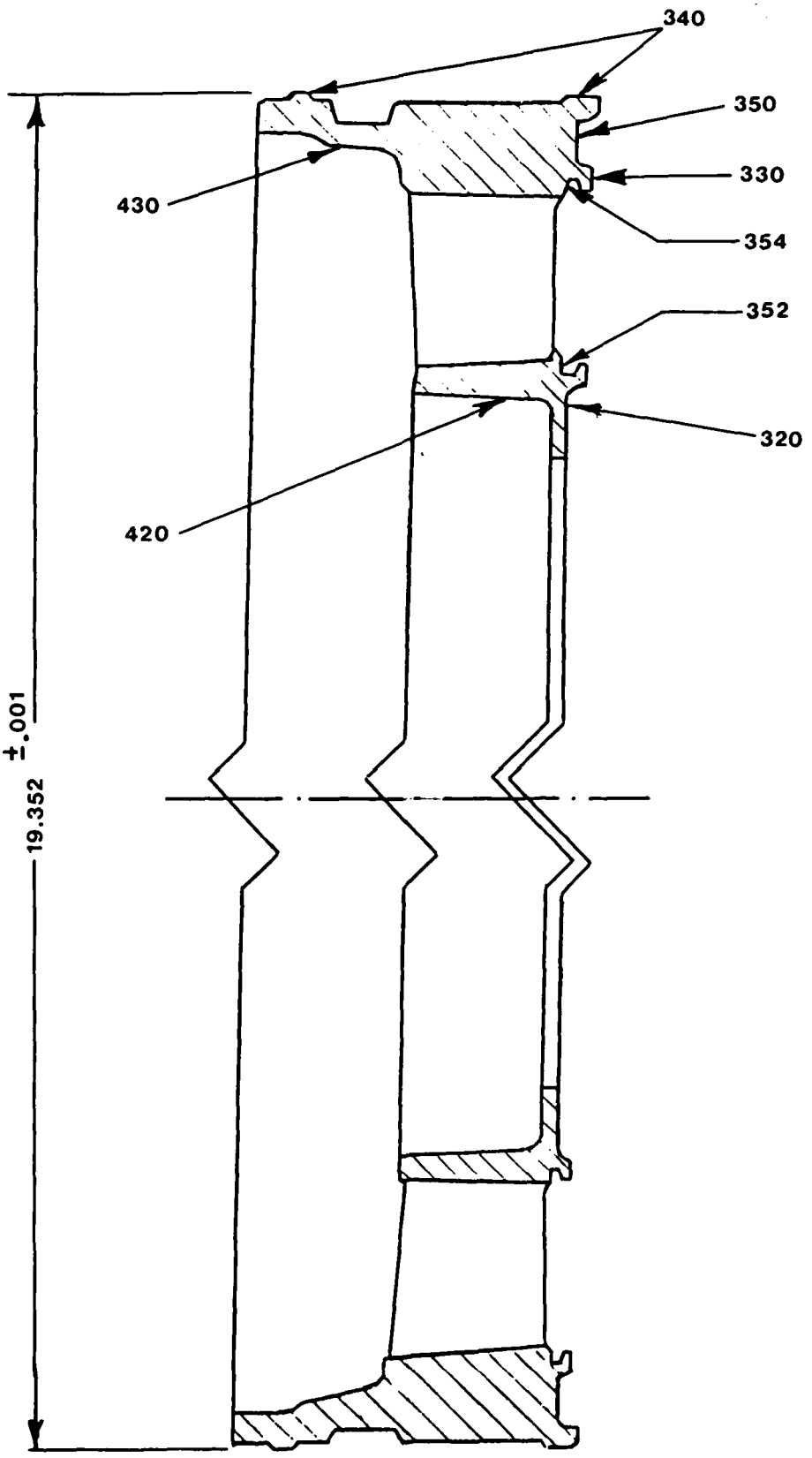

FIG 2

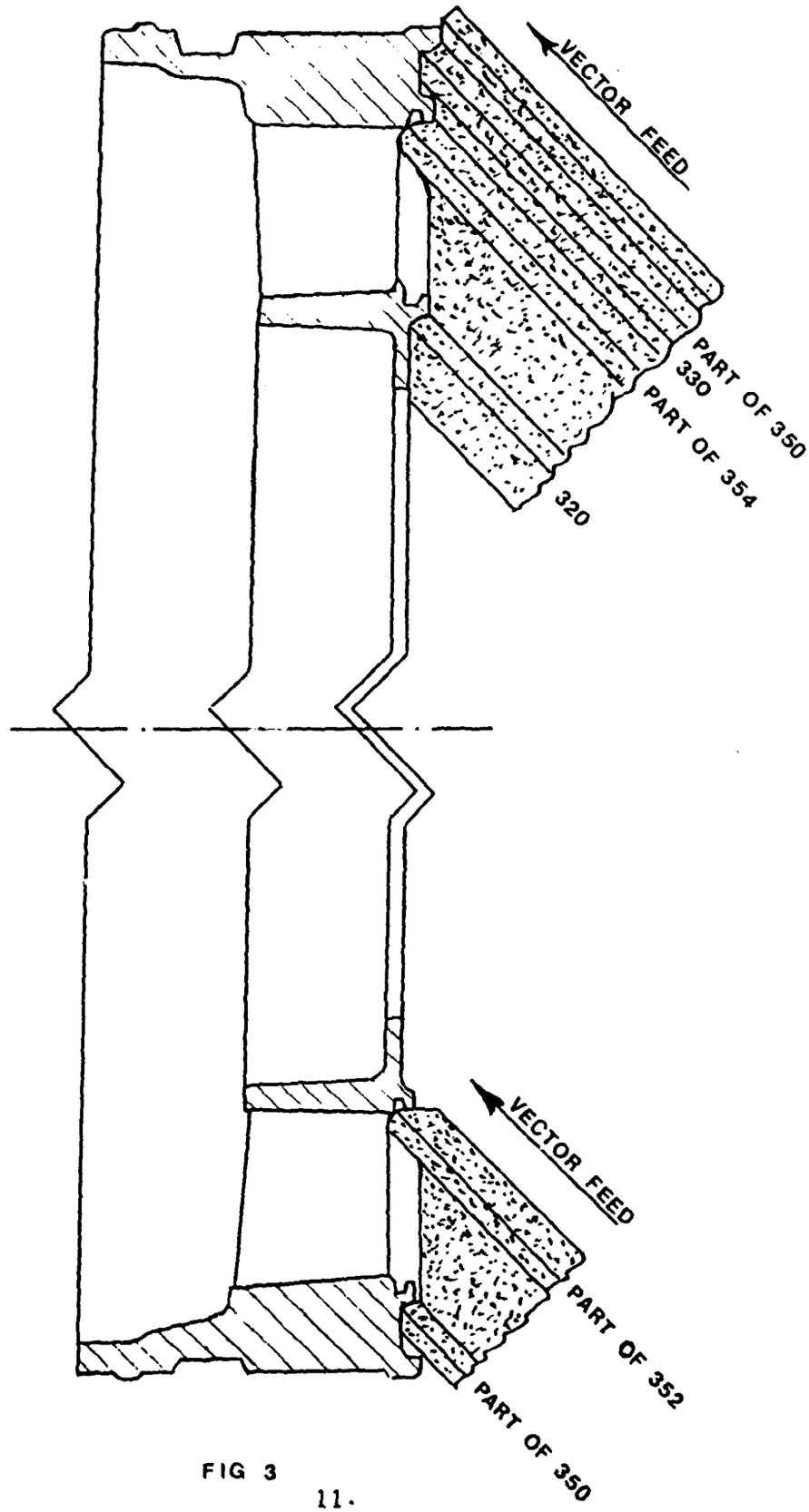
VECTOR FEED
PART OF 350
330
PART OF 354
320
VECTOR FEED
PART OF 352
PART OF 350

FIG 3

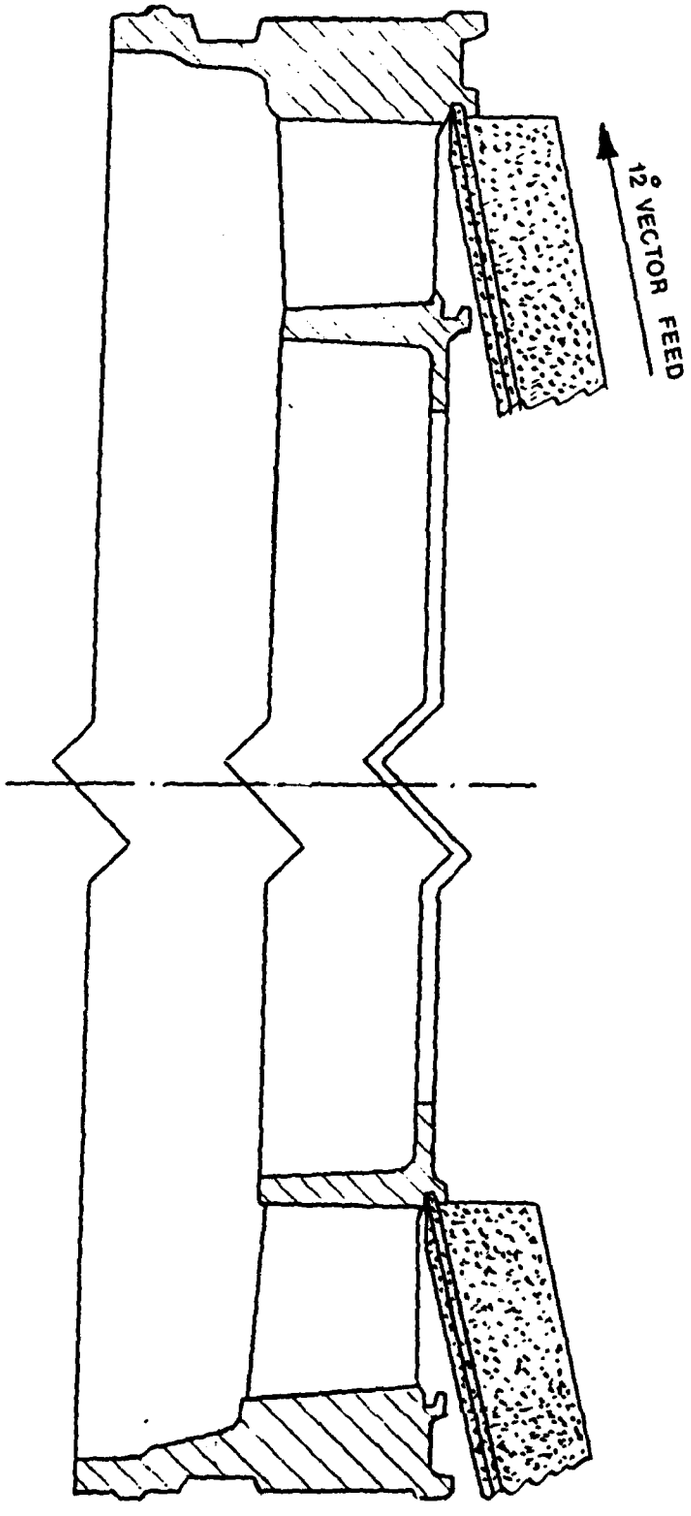

FIG 4

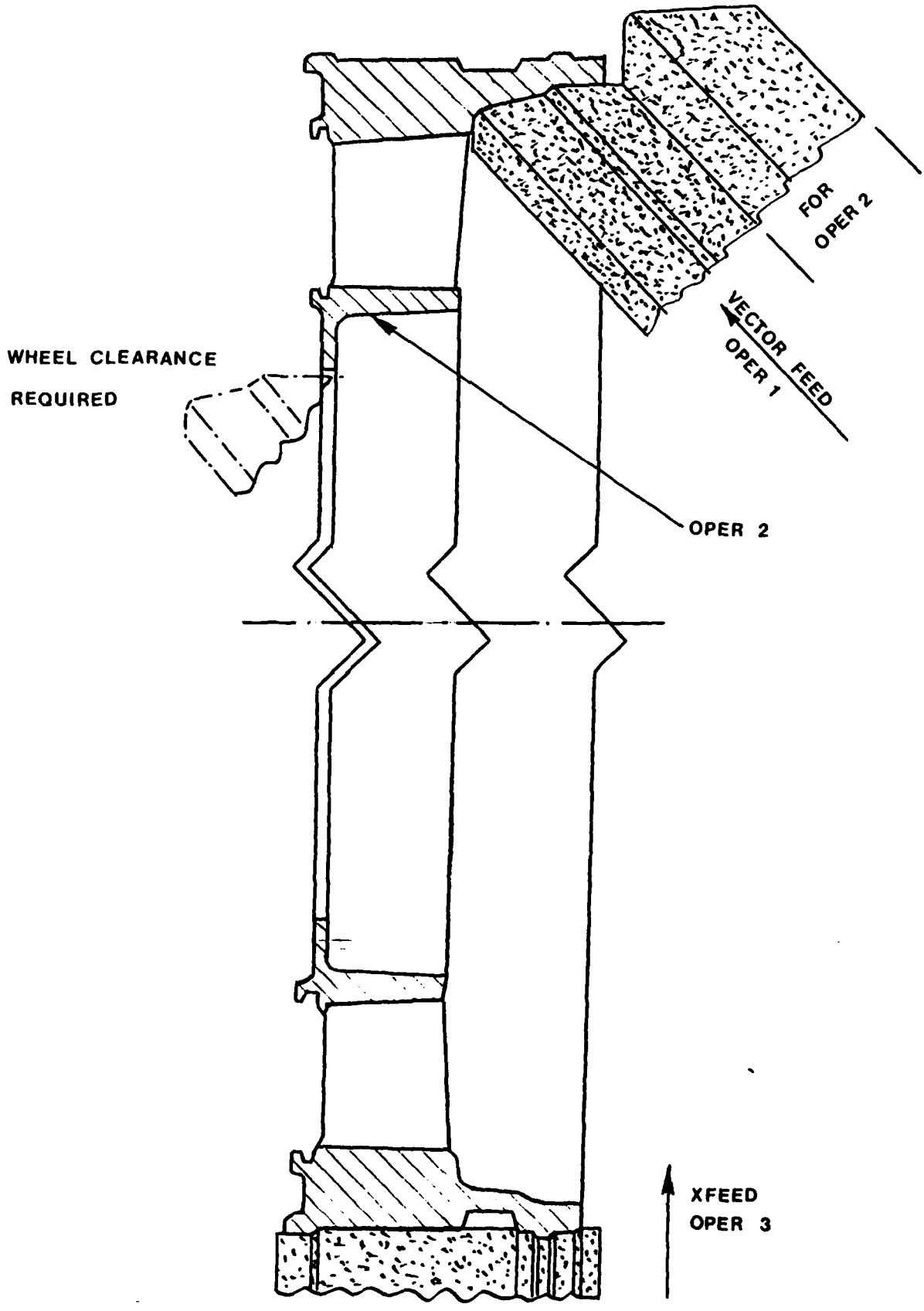
FOR
OPER 2
VECTOR FEED
OPER 1
WHEEL CLEARANCE
REQUIRED
OPER 2
XFEED
OPER 3

FIG 5

With the CNC multioperation method using two wheelheads on the same cross slide, the number of required machine tools is reduced from four to one, setups are reduced from five to three, and the machining time reduced from 9.37 hours to .96 hours as summarized in Table 1. Setup No. 1 is shown in Fig. 3 with one wheel performing operations 320, 330, part of 354 and part of 350 as operation 1, and the other head (not simultaneously) performing part of 350 and part of 352 as operation 2. The operation times for conventional workspeeds are given in Table 2. (Further reduction by creep grinding is discussed later.) Setup No. 2 is shown in Fig. 4 with both heads grinding simultaneously. Operation times are given in Table 3. Simultaneous operation of both heads can be achieved in this instance because of the relatively wide tolerance of ± .003 inches on the depth of the grooves. Setup No. 3 is shown in Fig. 5 where operations 430 and 420 are performed as operations 1 and 2 with one head, and operation 340 is performed subsequently with the second head as operation 3. Table 4 gives the operation times.

From the comparison of CNC multioperation grinding with two heads on a single cross slide with current methods outlined in Table 1, it can be seen that significant reduction in machining time can be achieved, not to mention the elimination of setup time. Setup times on large machines may take as long as 16 hours. Tooling costs may also be reduced as the number of setups is reduced.

3.0 MULTIOPERATION GRINDING--TWO WHEELHEADS--SEPARATE SLIDES

Large diameter parts often require wheelheads on separate slides. It may also be desirable to perform grinding operations with both heads and slides simultaneously. The "Vane-Cluster Assembly-3rd Stage" shown in Fig. 6 is another example where significant savings can be achieved by multioperation grinding. Eighteen of these Cluster Assemblies are mounted on the table of a vertical grinding machine to generate an O.D. of 44.67 inches along with the other surfaces shown in Fig. 6. Figure 7 shows the configuration of a typical large vertical grinding machine with the left-hand head arranged for O.D. grinding and the right-hand head for I.D. grinding. Current processing methods use the L.H. head to grind operation 40 in one setup. In another setup the O.D. of operation 50 is ground with the L.H. head while the R.H. head grinds the I.D. A third setup is used with the L.H. head roughing out part of operation 60 and the R.H. head finishing the groove of operation 60 to full depth. Operation 70 is performed in a fourth setup on a B&S surface grinder.

With the CNC multioperation method proposed here, assuming fixturing conditions can be satisfied, only one setup would be made. The L.H. head would be set up to grind operation 40, and the O.D. on operation 50 as shown in Fig. 8, thereby combining two operations into one.

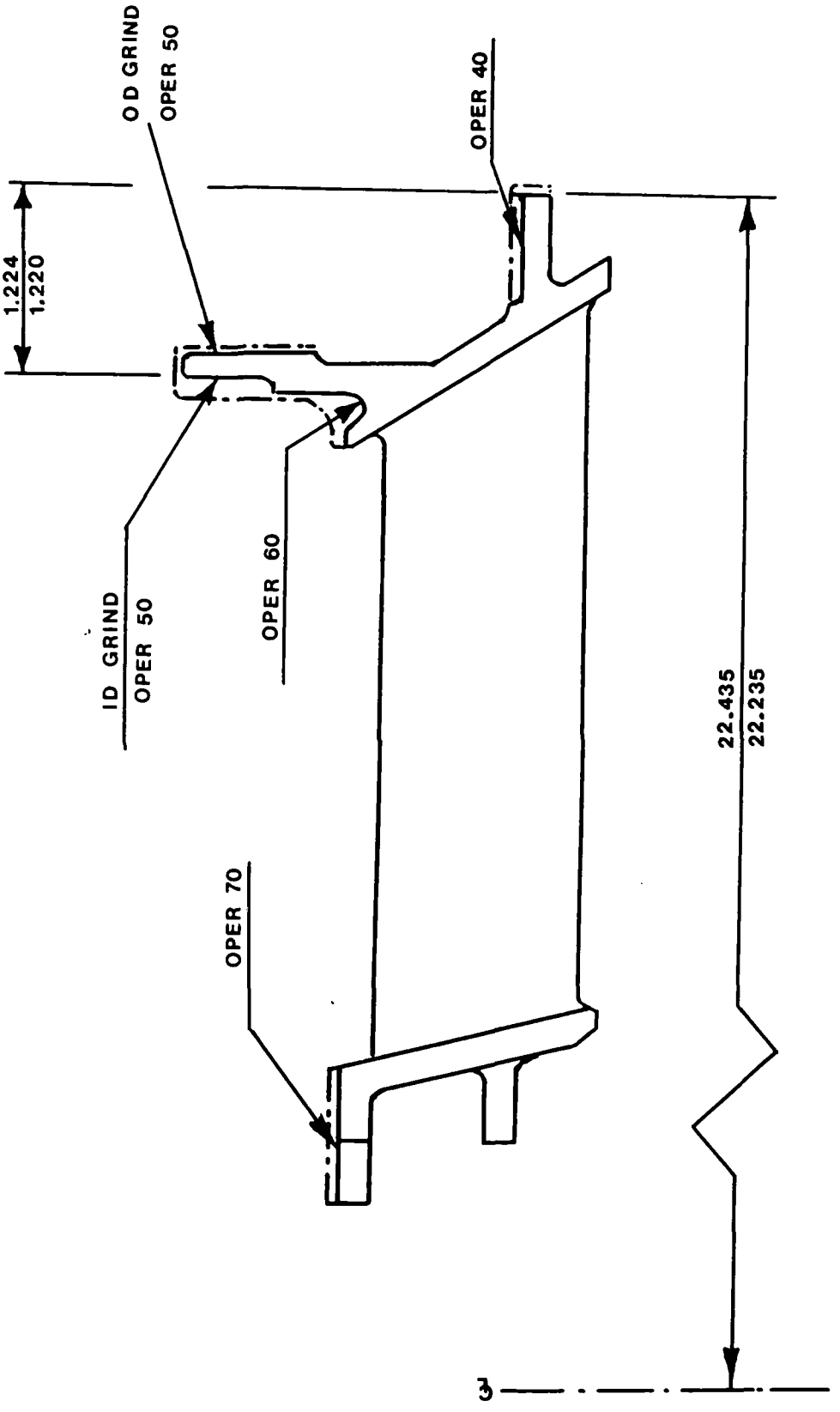
OD GRIND
OPER 50
OPER 40
1.224
1.220
ID GRIND
OPER 50
OPER 60
OPER 70
22.435
22.235
3

FIG 6

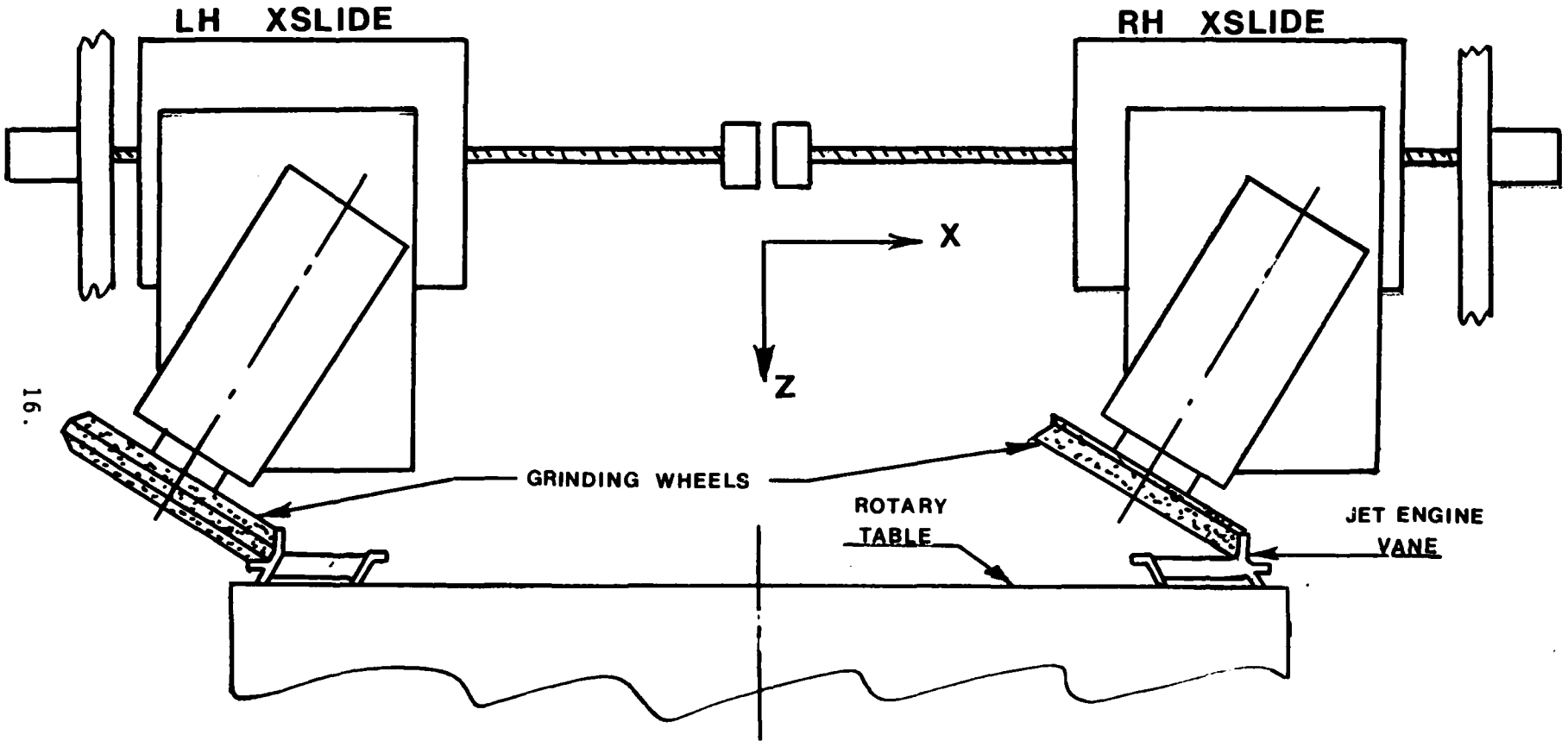
LH XSLIDE
RH XSLIDE
X
Z
GRINDING WHEELS
ROTARY TABLE
JET ENGINE VANE

FIG 7

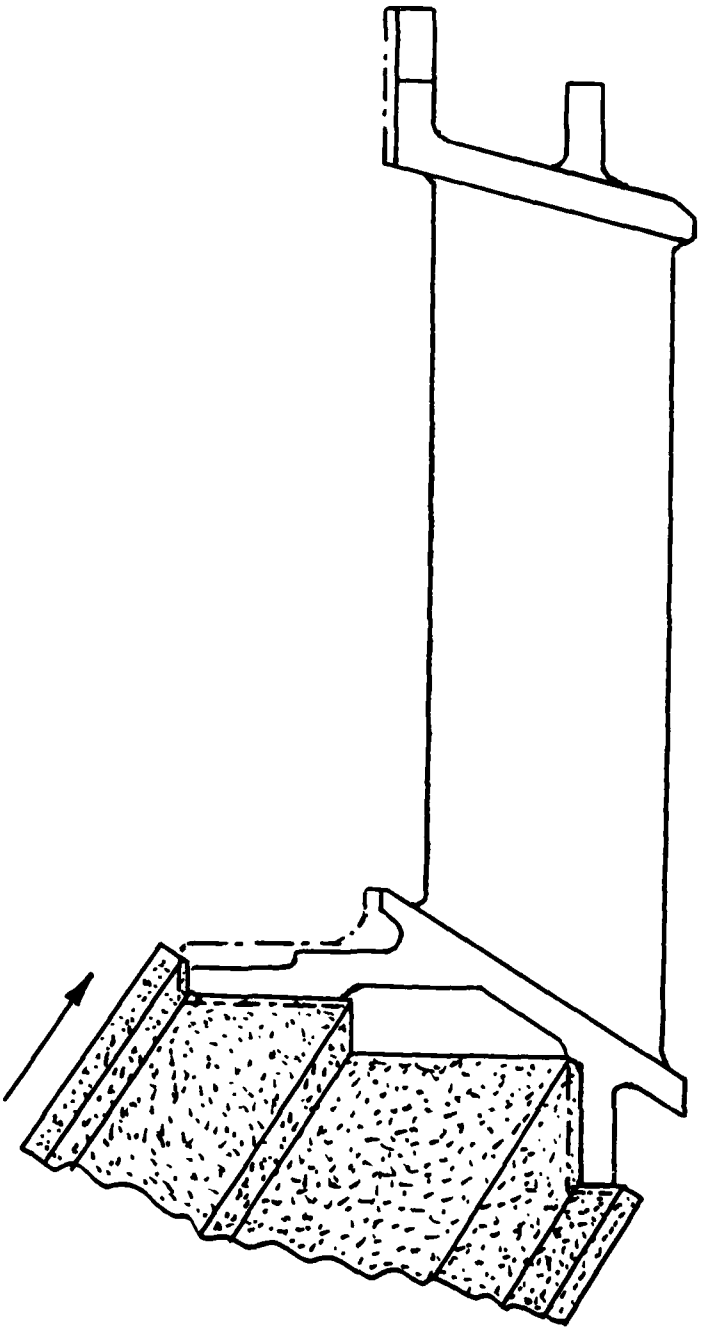

FIG 8

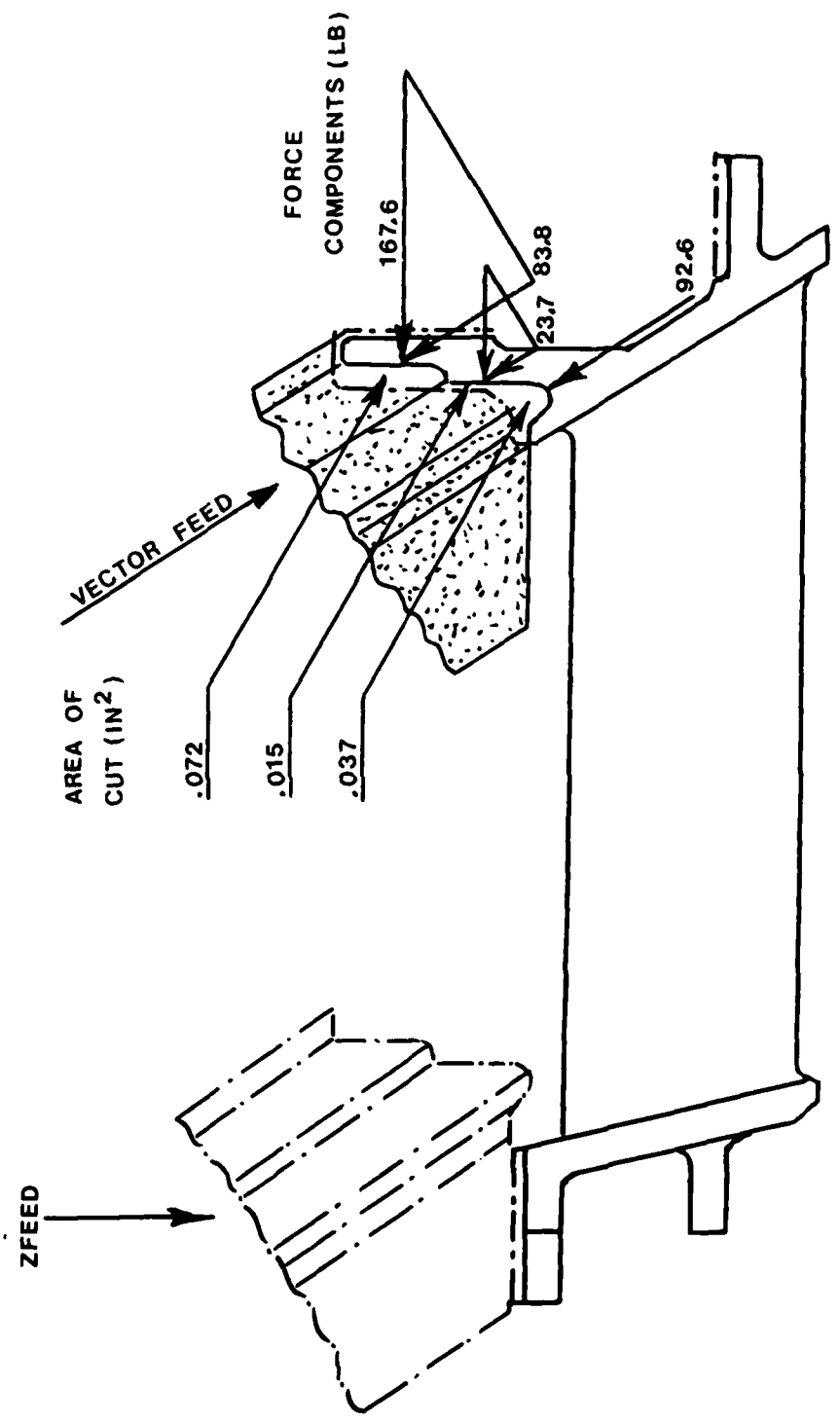
FORCE COMPONENTS (LB)
167.6
83.8
23.7
92.6
VECTOR FEED
AREA OF CUT (IN^2)
.072
.015
.037
ZFEED

FIG 9

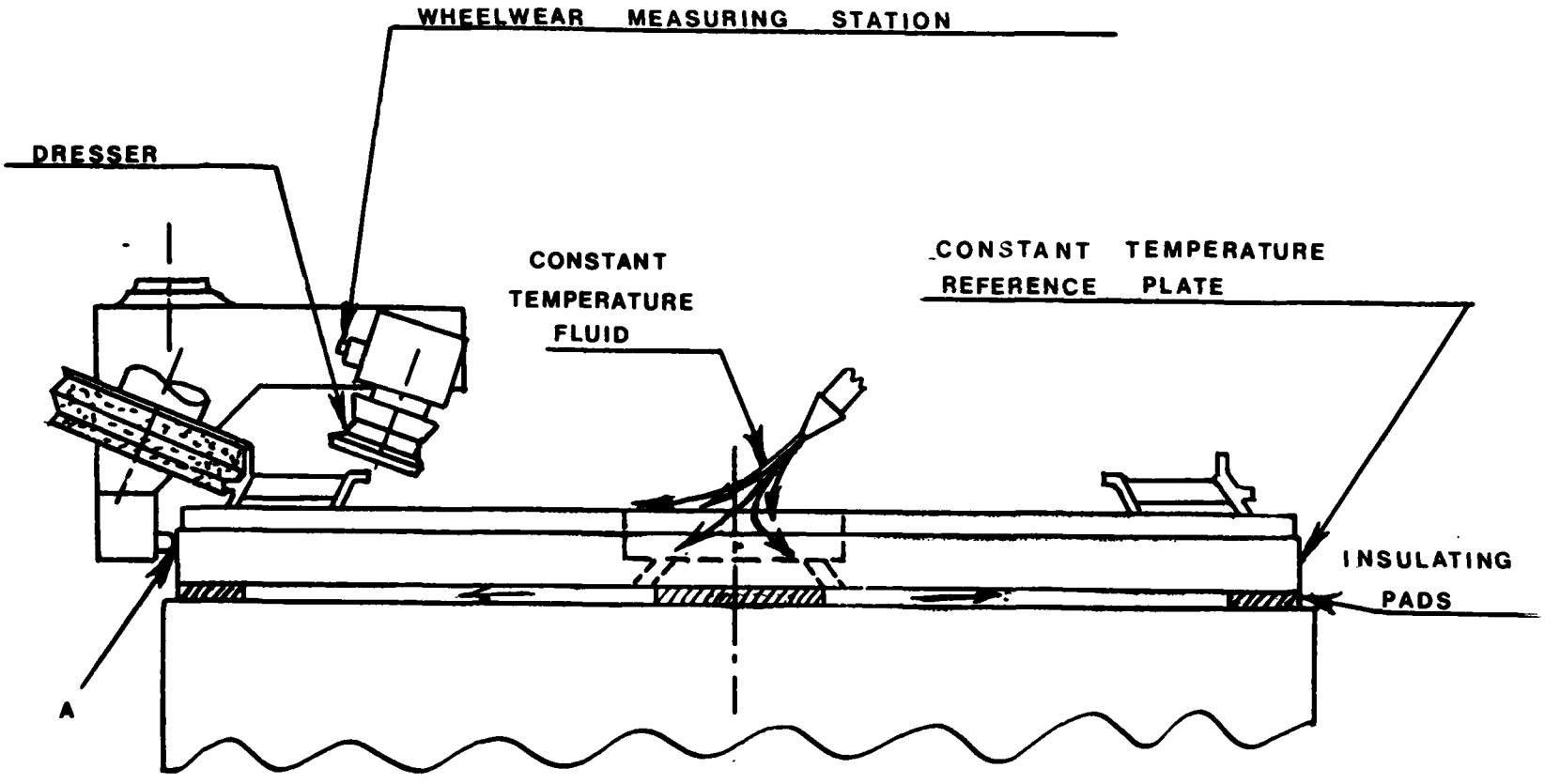
WHEELWEAR MEASURING STATION
DRESSER
CONSTANT TEMPERATURE FLUID
CONSTANT TEMPERATURE REFERENCE PLATE
INSULATING PADS
A

FIG 10

The I.D. part of operation 50 and operation 60 would also be combined and performed with the R.H. head simultaneously with the O.D. operation as illustrated by the vector feed in Fig. 9. At the conclusion of this operation (50,60) the R.H. head would index into position for executing operation 70 by performing a Z feed.

Table 5 summarizes these methods where two machines and four setups are required with the current method while one machine and one setup is required in the suggested method. Setup times for large grinders can vary from 3 hours to 16 hours with 8 hours as a reasonable average. Reducing the number of setups not only saves setup time, but also reduces tooling costs, such as diamond dressing rolls. In addition, the machining time from Table 5 is reduced from 296.8 min. for the current method to 101.8 min. for the CNC multioperation method.

3.1 AUTOMATIC PRECISION SIZING

The present method of sizing the various surfaces on the vanes generally requires the operator to interrupt the operation; to make a measurement of the remaining stock; to enter this information into the control, and to proceed to finish grind to final size. It would be desirable to have the machine automatically hold size directly without the attention of an operator thereby approaching untended operation. With multioperation grinding it is impractical to use "in-process" gaging because of the many surfaces generated. Therefore, it is necessary for the machine and its control to provide automatic precision sizing. Size errors can be caused by (1) Thermal Expansion (2) Elastic Deflection of the machine components (3) Variable amounts of wheelwear, and (4) Inaccuracies of Machine Movements. Methods for eliminating or greatly reducing Thermal Expansion errors are presented below. Methods for reducing deflection errors and wheelwear errors are presented in Section 6.

3.2 THERMAL EXPANSION ERRORS

The cross slides on large vertical grinders are typically driven by independent Servo motors and Ball Screw Drives as illustrated in Fig. 7. The origin of the X coordinate of each system is implicitly located at the corresponding ball screw thrust bearings or a limit switch nearby. On large machines only a few degrees rise in temperature can cause significant thermal expansion in the ball screws, columns and structure resulting in size errors. Figure 6 shows that a tolerance of ± .002 in between the I.D. grind of operation 50 (R.H. head) and the O.D. grind of operation 40 (L.H. head) is required. This means that a common stable reference system is required to precisely coordinate the movements of both heads.

The effect of thermal expansions in the machine structure and ball screws can largely be eliminated by using the dresser as a sizing reference and by insuring that the dresser is stably located in relation to the workpiece or table centerline. In this way, the wheel, once it is dressed, must move a specified distance from the dresser to produce a precision size. Thermally caused size errors are reduced to the thermal expansion of that section of the the ball screw involved in moving this short distance. Therefore, the dresser should be located as close as possible to the size position.

3.3 COMMON REFERENCE SYSTEM FOR DRESSERS

To construct a stable reference system a constant temperature is required. A temperature-controlled coolant system is probably the most convenient constant temperature reference. Figure 10 illustrates a diamond roll dresser mounted on a trunnion permitting it to be swung in over the workpiece and positioning the dresser roll relative to the work centerline. The stop A locates on the constant temperature reference plate which is bolted to the rotary table at the center through an insulating pad. Constant temperature cutting fluid bathes both top and bottom surfaces of the reference plate maintaining it at constant temperature. The rotary table is free to expand under the insulating pads due to bearing and table drive heat without deforming the reference plate. The grinding wheel comes into position in front of the trunnion and dresser bracket, and may move alternately back and forth from its grinding position to its dressing position. In some cases it may be desirable to replace the stop A with a displacement transducer and provide a fixed stop against the base to avoid the sliding contact stop at A. Then the displacement transducer can be interfaced to the computer control which, in turn, can compensate for thermal dresser movements relative to the reference plate. A similar diamond dress roll, and trunnion support would also be provided for the R.H. head thereby referencing it to the common reference plate. In this way, thermal size errors can be largely eliminated. Thermal displacements in other parts of the machine have no effect on size as long as the wheels contact the dresser rolls during dressing. In effect, the thermal displacements are absorbed in the "Compensation for Wheelwear" movement.

4.0 PRINCIPLES OF GRINDING

The success of the grinding operations described above is critically dependent upon the grinding wheel's ability to remove stock and to maintain its form. It is important, therefore, to develop relationships for stock-removal rate, wheelwear rate,

surface finish and surface integrity in terms of feedrate, grinding force, wheelspeed, workspeed, etc. Recent trends in Europe and the U. S. toward "Creep Feed" grinding indicate improved stock-removal rates, and reduced wheelwear using the "Creep Feed" method. Accordingly, it is desirable to relate and compare "Creep Feed" grinding with normal workspeed grinding. In order to do this the following sections define and present important grinding variables.

4.1 Input-Output Variables

Although many grinding operations perform satisfactorily, occasional undesired results are sometimes produced; viz, thermal damage, size scatter, fluctuating taper, variations in surface finish, form errors, etc. These variations in output variables are caused by variations in certain grinding process variables which are not being properly controlled. It is important to distinguish between inputs to the grinding machine, inputs to the grinding process and outputs from the grinding process as illustrated in Fig. 11. The inputs to the grinding machine consist of the various machine settings as well as stock variations, stock runout and hardness variations. These inputs to the machine cause certain wheelwork interface forces to be generated. These forces, along with the wheel sharpness, act as inputs to the grinding process (that which occurs at the wheelwork contact zone). Outputs from the grinding process are listed on the right in Fig. 11. In order to obtain certain desired outputs it is helpful to understand the relationship of the various outputs to the inputs. These relationships are developed in the following sections.

4.2 The Wheelwork Interface

The grinding process takes place at the wheelwork interface. In cylindrical plunge-grinding operations, the interface force intensity (normal force per unit width of contact) is uniformly distributed over the face of the wheel. Accordingly, plunge grinding is the simplest type of grinding as illustrated in Fig. 12. The feedrate $\bar{v}_f$ is applied to the cross slide of the machine. At the moment the wheel contacts that workpiece, the interface force intensity is zero. As the cross slide continues to move, the "springs" in the system compress, generating some interface force intensity F'_n. This causes the wheel and work to mutually "machine" each other, the radius of the workpiece decreasing at the rate $\bar{v}_w$, the radius of the wheel decreasing at the rate $\bar{v}_s$, and the deflection x increasing at the rate $\dot{x}$, thus:

$$\bar{v}_w + \bar{v}_s + \dot{x} = \bar{v}_f \qquad (1)$$

The feedrate of the cross slide $\bar{v}_f$ only equals the plunge-grinding velocity $\bar{v}_w$ when the wheelwear $\bar{v}_s$ is negligible and $\dot{x} = 0$ (the steady state).

GRINDING PROCESS RELATIONSHIPS

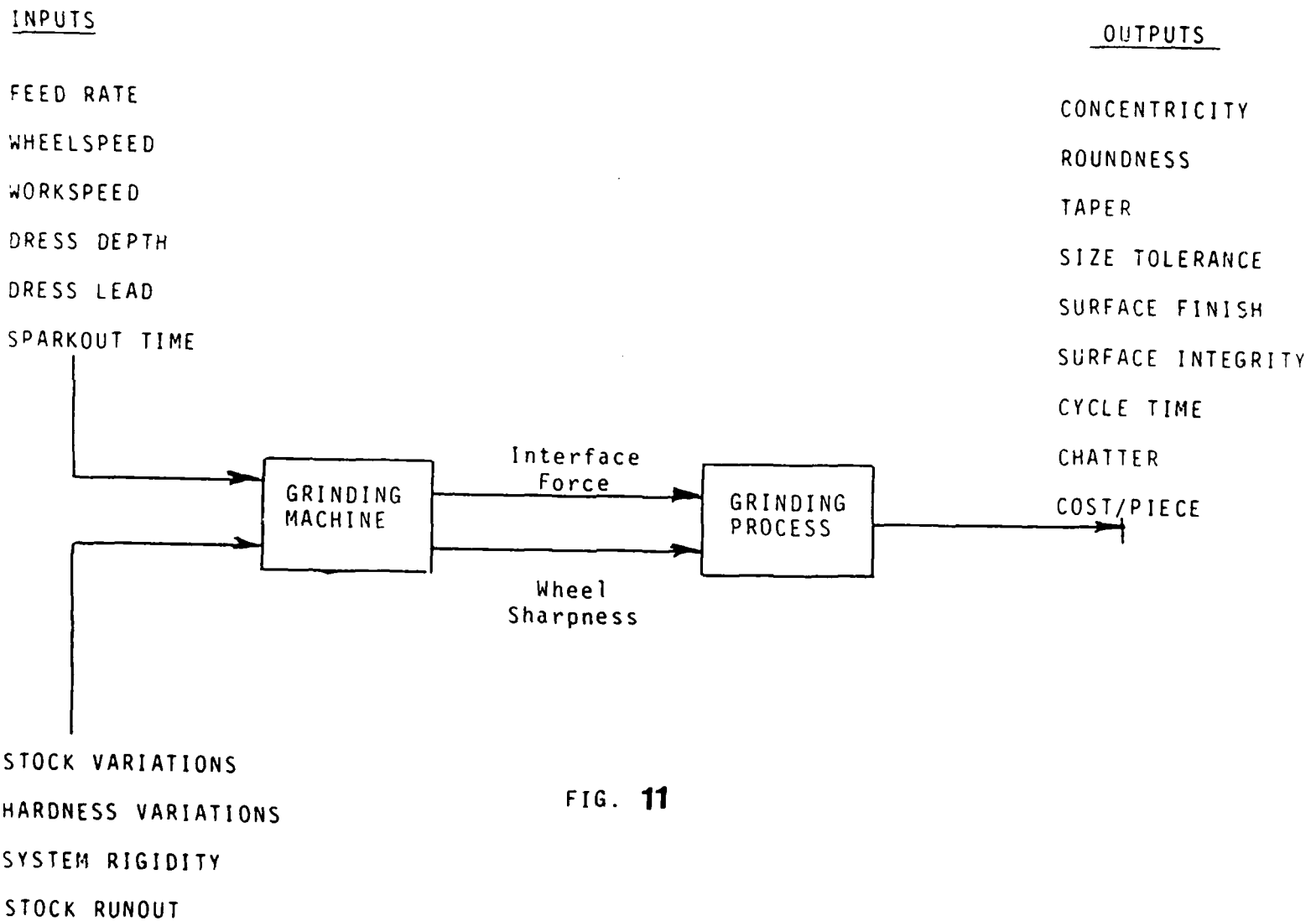

FIG. 11

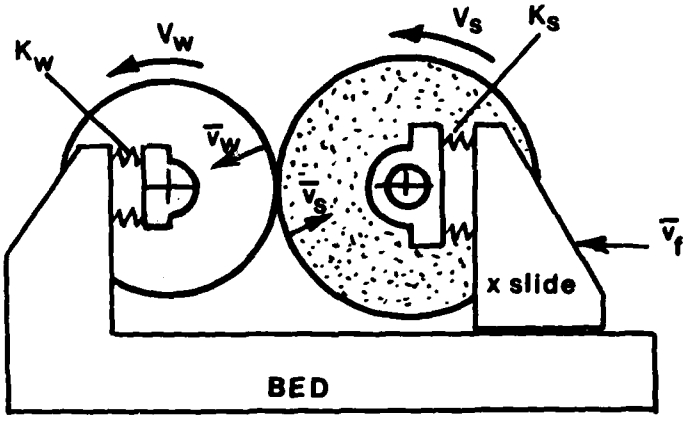
K_w
V_w
V_s
K_s
$\bar{v}_w$
$\bar{v}_s$
$\bar{v}_f$
x slide
BED

FIG 12

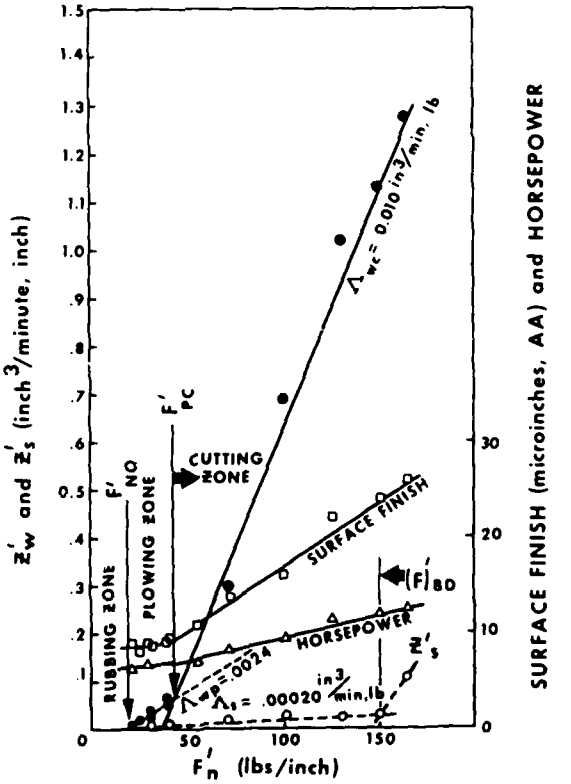
$\bar{z}'_w$ and $\bar{z}'_s$ (inch^3/minute, inch)
F'_n (lbs/inch)
SURFACE FINISH (microinches, AA) and HORSEPOWER
RUBBING ZONE
PLOWING ZONE
CUTTING ZONE
F'_{PC}
F'_{NO}
SURFACE FINISH
HORSEPOWER
$(F'_n)_{80}$
$\bar{z}'_s$
Λ_{wc} = 0.010 in^3/min. lb
Λ_{sc} = .0024
Λ_s = .00020 in^3/min.lb

FIG 13

$$D_E = \frac{D_s}{1 - D_s/D_w} = \frac{3.6\,in}{1 - 3.6/4.0} = 36.\ inch$$

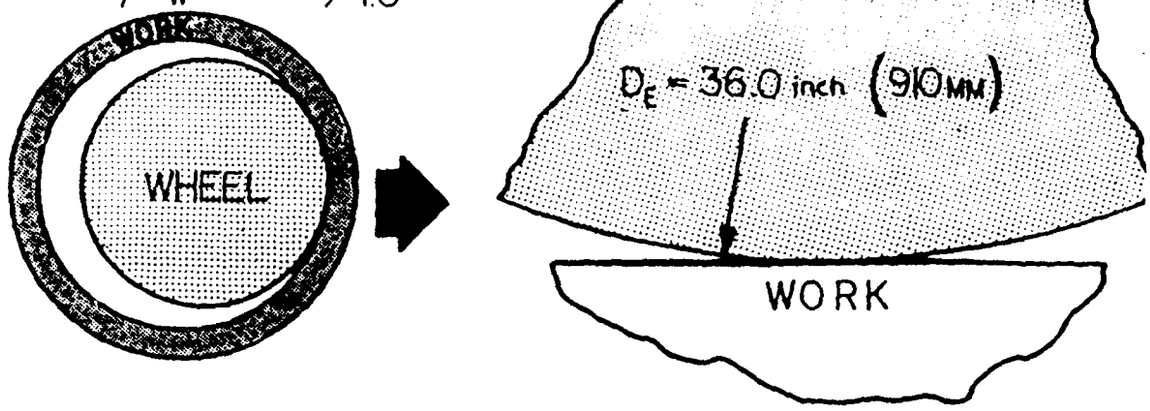

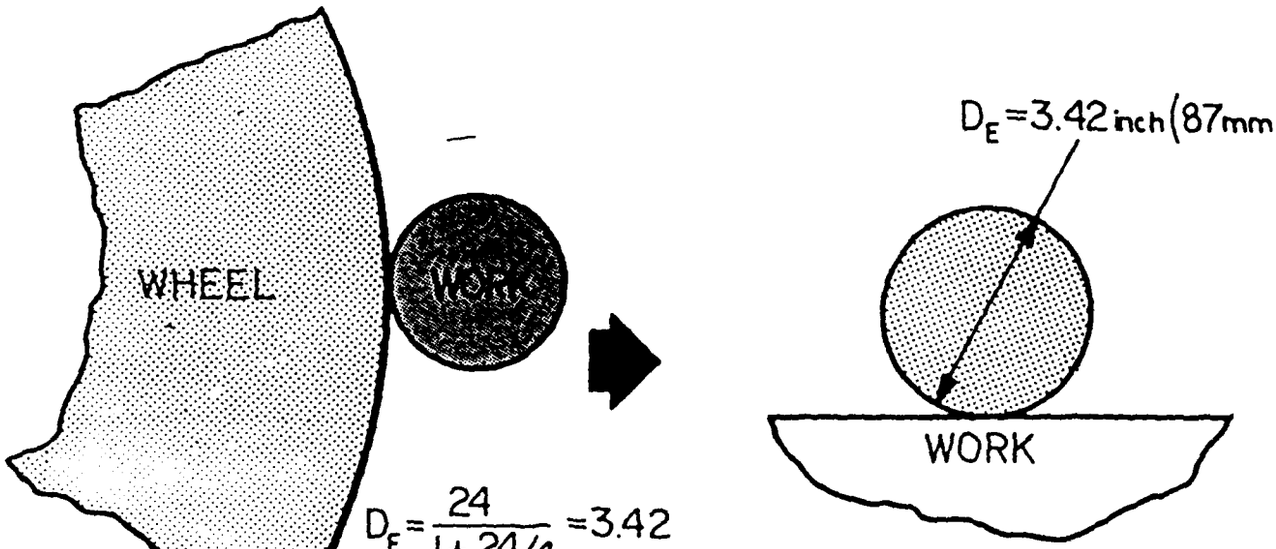

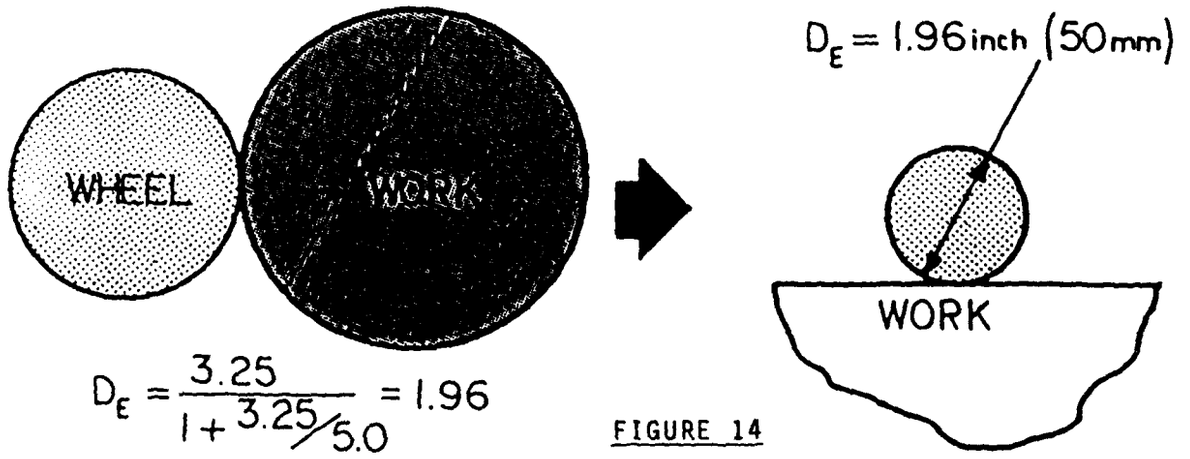

FIGURE 14

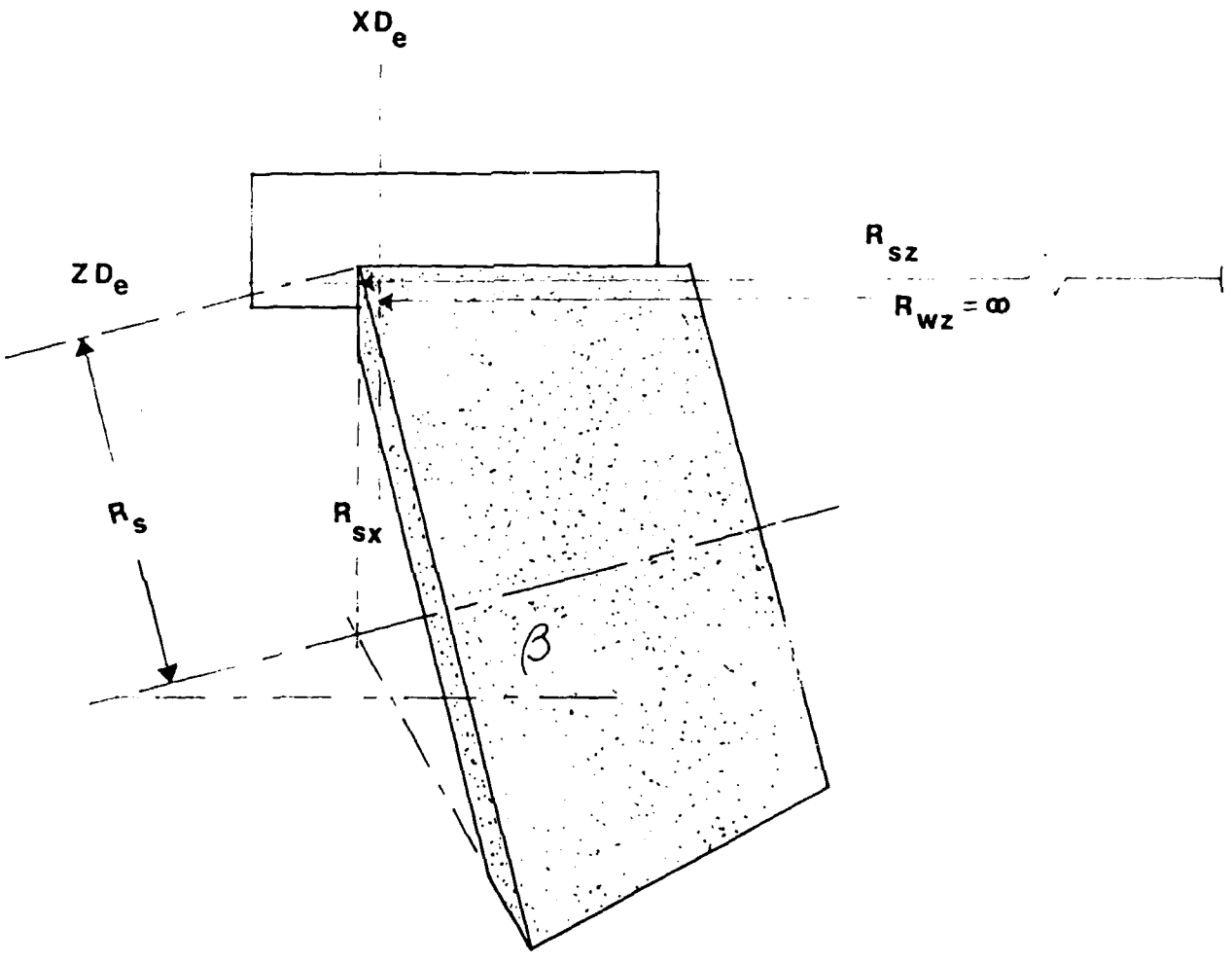

Figure 15

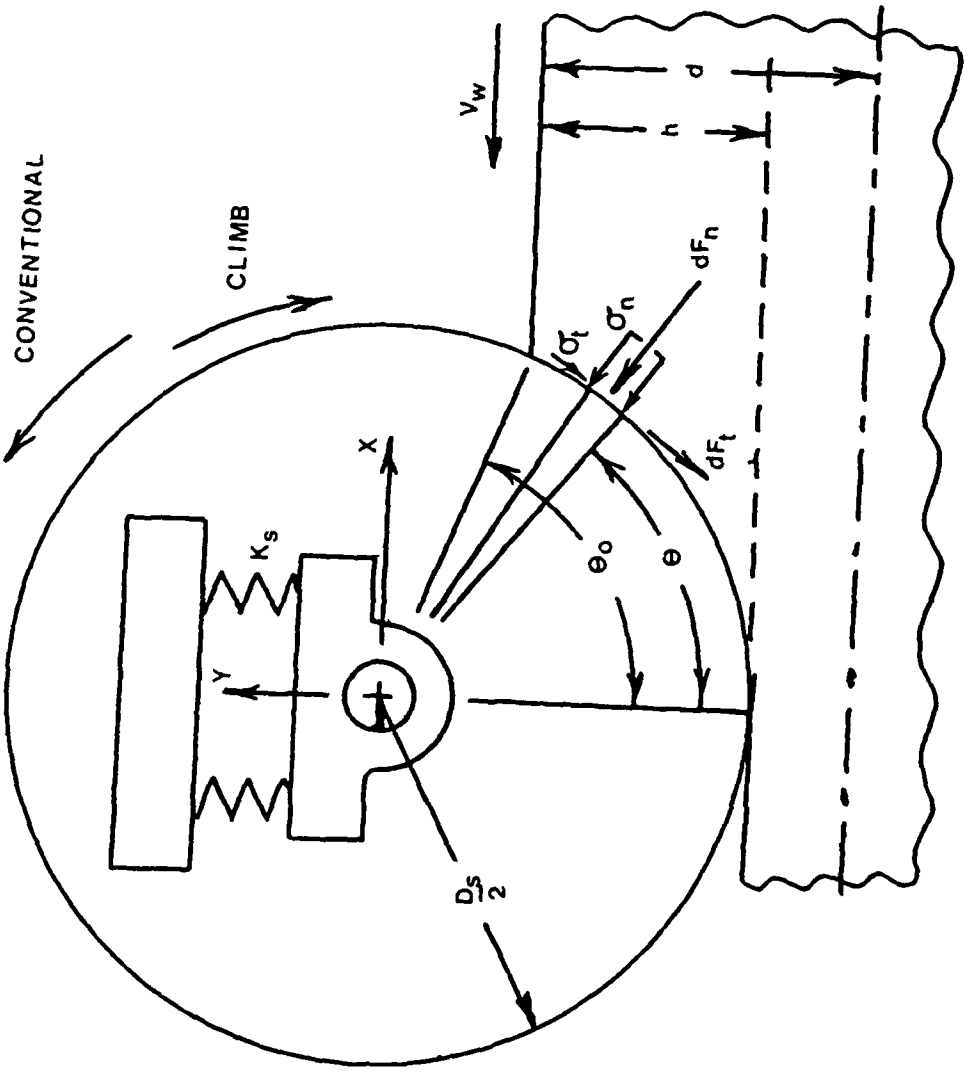
CONVENTIONAL
CLIMB
V_w
d
h
dF_n
σ_t
σ_n
dF_t
X
Y
K_s
e_o
e
$\frac{D_s}{2}$

FIG 16

The volumetric rates of stock removal Z'_w and wheelwear Z'_s per unit width of contact:

$$Z'_w = \pi D_w \bar{v}_w \qquad (2)$$

$$Z'_s = \pi D_s \bar{v}_s \qquad (3)$$

are plotted against the normal interface force intensity in Fig. 13, resulting in a "Wheelwork Characteristic Chart" which shows how a given wheelwork pair machine each other. The stock-removal curve Z'_w (solid dot) has a "Rubbing Region" at force intensities below F'_{th} the "Threshold Force Intensity"; a "Plowing Region" for force intensities between F'_{th} and F'_{pc}, the "Plowing-Cutting Transition"; and, a "Cutting Region" above F'_{pc} (2). In the cutting region, the abrasive grits remove chips, in the usual way; in the plowing region they remove material by causing lateral plastic flow, and highly extruded ridges to be formed along each side of the scratch, these ridges being removed by subsequent grits. The plowing region is important in obtaining good surface finishes. The cutting region is important in rounding up the workpiece and fast stock removal.

The slope of the Z'_w curve is called the "Work Removal Parameter", WRP, or sometimes, Λ_w, and is indicative of the "Sharpness" S, of the grinding wheel, defined as:

$$S = \frac{WRP}{V_s} \qquad (\frac{m^2}{N}) \qquad (4)$$

which represents the cross-sectional area of a hypothetical ribbon of material being removed from the workpiece per unit normal force. The sharpness of grinding wheels is one of the most important variables in the grinding process, and is frequently most difficult to control in practical grinding operations. Its value may vary 400% to 500%, causing size, taper, surface finish, and surface integrity problems.

The wheelwear curve Z'_s, in Fig. 13, rises gradually at low force intensity and then turns sharply upward (around 28 N/mm (150 lb/in) in this case), at the so-called "Breakdown Force Intensity" F'_{bd}. Precision grinding cycles must operate between F'_{th} and F'_{bd}. Curves for Surface Finish and Power can also be shown on the Wheelwork Characteristic Chart.

4.3 Wheelwork Conformity

The difference in curvature of the wheel and work in the contact region has some effect on the cutting action at the wheelwork

interface. The difference of curvature for internal or external grinding can be related to surface grinding by considering an "Equivalent Diameter" D_e of a surface grinding wheel having the same difference of curvature as the internal or external operation.

The "Equivalent Diameter" D_e illustrated in Fig. 14 is given by:

$$\frac{2}{D_e} = \Delta = \frac{2}{D_s} \mp \frac{2}{D_w} \qquad (5)$$

$$D_e = \frac{D_w D_s}{D_w \pm D_s} \qquad (6)$$

where the + or - sign is used for external or internal grinding. With this parameter, internal, external, and surface grinding can be related.

In grinding shoulders with wheels inclined at the angle β, the radii of curvature of the abrasive wheel in the X and Z directions shown in Fig. 15 are:

$$R_{sx} = \frac{D_s}{2\cos\beta} \qquad (7)$$

$$R_{sz} = \frac{D_s}{2\sin\beta} \qquad (8)$$

so that:

$$XD_e = \frac{D_w\left(\frac{D_s}{\cos\beta}\right)}{D_w \pm \left(\frac{D_s}{\cos\beta}\right)} \qquad (9)$$

$$ZD_e = \frac{D_s}{\sin\beta} \qquad (10)$$

The preceding equations are valid for conventional cylindrical and surface grinding, but they are not valid for "Creep Feed" grinding. In "Creep Feed" grinding the workspeed is very slow, and the wheel is set to take the full amount of stock in a single pass as illustrated in Fig. 16. Under these conditions the grinding wheel tends to grind its own curvature into the workpiece regardless of the curvature of the work. The surface in the immediate contact zone is a trochoidal surface as shown by Hahn (1), and it is the difference in curvature Δ, between the wheel and this trochoidal surface that affects the grinding

action. This difference in curvature from reference (1) is:

$$\Delta_i = \frac{2}{D_s}\left[\frac{\left(\frac{D_w}{D_s}-1\right)\left(\frac{D_w}{D_s}+\frac{2N_s}{N_w}\right)}{\left(\frac{D_w}{D_s}+\frac{N_s}{N_w}\right)^2}\right] \qquad (11)$$

and the corresponding Equivalent Diameter D_e is:

$$D_e = \frac{2}{\Delta_i} \qquad (12)$$

In "Creep Feed" grinding, very large values of D_e occur. Their affects will be discussed in Section (5.3).

4.4 Basic Plunge-Grinding Relations for Conventional Cylindrical Grinding*

Stock removal, wheelwear, surface finish, power and force relationships can be developed from the Wheelwork Characteristic Chart illustrated in Fig. 13. Neglecting the plowing region in Fig. 13 for simplicity, the stock-removal relation is:

$$Z'_w = WRP\ (F'_n - F'_{th}) \text{ or:} \qquad (13)$$

$$\pi D_w \bar{v}_w = WRP\ (F'_n - F'_{th}) \text{ or:} \qquad (14)$$

$$\bar{v}_w = \frac{WRP(F'_n - F'_{th})}{\pi D_w} \qquad (15)$$

Equation 15 gives the plunge-grinding velocity in terms of the normal interface force intensity.

When the wheelwear rate is negligible ($\bar{v}_s < \bar{v}_w$) and a steady state of deflection exists ($\dot{x} = 0$) equation 1 becomes:

$$\bar{v}_w = \bar{v}_f \qquad (16)$$

Equation 15 can be solved for F'_n with $\bar{v}_f$ replacing $\bar{v}_w$, thus:

$$F'_n = \frac{\pi D_w \bar{v}_f}{WRP} + F'_{th} \qquad (17)$$

*Primed quantities signify per unit width

This gives the induced force intensity generated by the feedrate $\bar{v}_f$ in the steady state.

The wheelwear curve Z'_s in Fig. 13, below F'_{bd}, may be approximated according to Lindsay (5) by:

$$Z'_s = WWP\ (F'_n)^2 \qquad (18)$$

$$\text{Where:}\quad WWP = .068 \times 10^{-9}\left[\frac{\ell^2\left(1+\frac{c}{\ell}\right) N_s\ D_s}{\left(\frac{D_e}{2.54}\right)^{1.2}/vol\,(vol)^{.85}}\right] \quad \left(\frac{mm^4}{min*N^2}\right) \qquad (19)$$

With this wheelwear parameter, WWP, wheelwear can be estimated for various grinding conditions.

The Breakdown Force Intensity F'_{bd} in Fig. 13 may be estimated for Al_2O_3 vitrified wheels (3) by:

$$F'_{bd} = 62.3(vol)^{.55}(D_e)^{.25} \quad (N/cm) \qquad (20)$$

Precision grinding cycles should be designed so that the induced force intensity lies below F'_{bd}.

The wheel depth-of-cut h (advance of wheel per work revolution) is given by:

$$h = \frac{\bar{v}_w}{N_w} \quad (\mu m) \qquad (21)$$

This relation permits all the results developed for cylindrical grinding to be applied to surface grinding operations at normal workspeeds.

The "Work Cutting Stiffness", K_c (normal force required to take unit depth-of-cut) is an important quantity governing the rate of rounding up, the sparkout time, and chatter behavior when compared to the "System Stiffness" K_m. It is given by:

$$K_c = \frac{F_n}{h} = \frac{V_w W}{WRP} \quad (N/mm) \qquad (22)$$

The dimensionless "Machining--Elasticity Number", α, formed by the ratio:

$$\frac{K_c}{K_m} = \alpha \qquad (23)$$

relates elastic effects in machining or grinding operations to the stiffness of the machine tool.

The Power P absorbed in the grinding process is:

$$P = F_t V_s \quad \left(\frac{N\ m}{sec}\right) \quad \text{(watts)} \qquad (24)$$

The ratio F_t/F_n varies between .3 for a dull wheel, and .7 for a sharp wheel with an average value of .5. Therefore:

$$F_t = .5F_n \qquad (25)$$

and:

$$P = 1/2\ F_n V_s \qquad (26)$$

Using Eq. 17 and neglecting the threshold force F_{th}

$$P = \frac{\pi\ D_w W\ V_s}{2\ WRP}\ \bar{v}_f \qquad (27)$$

gives the power required for any feedrate $\bar{v}_f$.

The "Specific Power" P_s using Eq. 13 and neglecting F'_{th} is:

$$P_s = \frac{P'}{Z'_w} = \frac{V_s}{2\ WRP} \quad \left(\frac{joules}{mm^3}\right) \qquad (28)$$

The "Time Constant" τ_o of a grinding system governs the time required to build up grinding force or sparkout. It depends upon the System Stiffness K_m and on the material being ground WRP (3).

$$\tau_o = \frac{\pi\ D_w W}{WRP\ K_m} \quad \text{(sec)} \qquad (29)$$

On materials exhibiting a plowing region, the time constant suddenly changes during a sparkout when the plowing region is encountered. The WRP in the plowing region is about 1/3 WRP in the cutting region.

The "G Ratio" giving the ratio of the volume of metal removed to the volume of abrasive consumed is generally a variable depending upon the particular operating force intensity. It is a valid ratio only in the case where the Z'_w vs. F'_n and the Z'_s vs F'_n relations are straight lines emanating from the origin in Fig. 13. Generally, this is not true.

4.5 Machinability Parameters in Grinding

The Work Removal Parameter, WRP, the Threshold Force Intensity in Eq. 13 and the Specific Power, are the principle factors governing machinability in grinding. Some typical values of WRP for various alloys are given in Fig. 17 ranging from around .06 for T15, to 1.5 (cumm/sec*N) for chrome cast iron. Values of WRP may be estimated for so-called "Easy-to-Grind" materials with Lindsay's (5) semiempirical equation:

$$WRP = .00958 \frac{\left(\frac{N_w D_w}{N_s D_s}\right)^{.15} \left(1+\frac{2c}{3\ell}\right) \ell^{.58} N_s D_s}{D_e^{.14} (vol)^{.47} d^{.13} (R_c)^{1.42}} \quad (cumm/min*N) \quad (30)$$

Values of WRP for "Difficult-to-Grind" materials are best obtained by measurement. Some typical values for T15 and M50 are shown in Figures 18 and 19. These figures also show Threshold Force Intensities F'_{th}. The Threshold Force is very important at large D_e, and often causes problems in rounding up, sizing, and obtaining consistent surface finish. The variation of F'_{th} with D_e for several wheel speeds is shown in Fig. 20.

The Specific Power P_s for AISI 52100,M50 and M4 at several wheel speeds, shown in Fig. 21 ranges from 7.7 for 52100 to 320 (HP/cu.in/min) for M4. The "Lindsay Chart" (4) in Fig. 22 shows the relation between P_s and WRP for Cast Iron, AISI 52100,M50 and M4. For each material, the arrows indicate the effect of increasing wheel speed. For Cast Iron increasing wheel speed reduces P_s and increases WRP, both parameters moving in a favorable direction. For M4, increasing wheel speed increases P_s and reduces WRP, both parameters moving in an unfavorable direction. Accordingly, M4 should be ground at low wheel speeds while Cast Iron at high wheel speed.

4.6 Surface Integrity

The generation of precision surfaces with good surface finish does not necessarily guarantee a surface free of thermal cracks, or residual tensile stress. Those detrimental effects are caused by localized high temperatures during the grinding operation. There is generally a threshold temperature above which thermal damage will result. If grinding conditions are adjusted to stay below this threshold, good surface integrity can be obtained. The principle factors determining the heat generated in grinding are the wheel speed,work speed, force intensity, D_e, and wheel sharpness, the latter being the most difficult to control. As the wheel dulls, the Sharpness, S, defined by Eq. 4 drops, thereby reducing WRP, which, in turn, causes a rise in F'_n according to Eq. 17. Both of these effects tend to raise grinding temperatures.

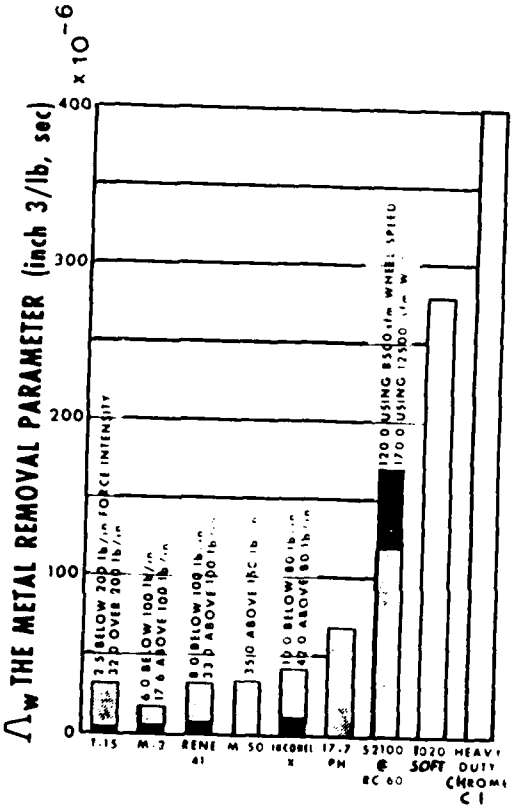
Λ_w THE METAL REMOVAL PARAMETER (inch 3/lb, sec) x 10^{-6}
400
300
200
100
0
M-2
RENE 41
M 50
INCONEL X
17-7 PH
52100 @ RC 60
SOFT
HEAVY DUTY CHROME

FIG. 17

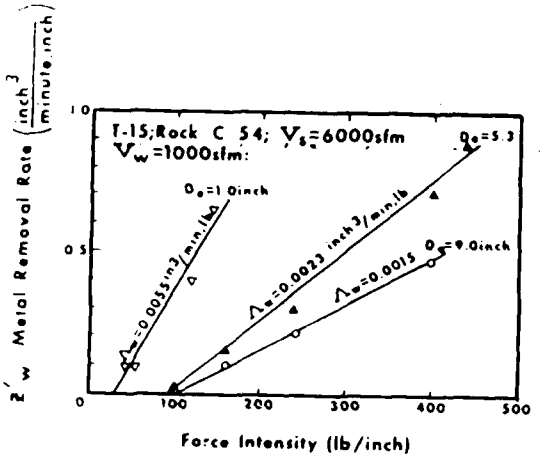
T-15;Rock C 54; V_s=6000sfm
V_w=1000sfm:
D_e=5.3
D_e=1.0inch
Λ_w=0.0055 inch³/min.lb
Λ_w=0.0023 inch³/min.lb
Λ_w=0.0015
D_e=9.0inch
Z'_w Metal Removal Rate (inch³/minute.inch)
Force Intensity (lb/inch)
0
0.5
1.0
100
200
300
400
500

FIG. 18

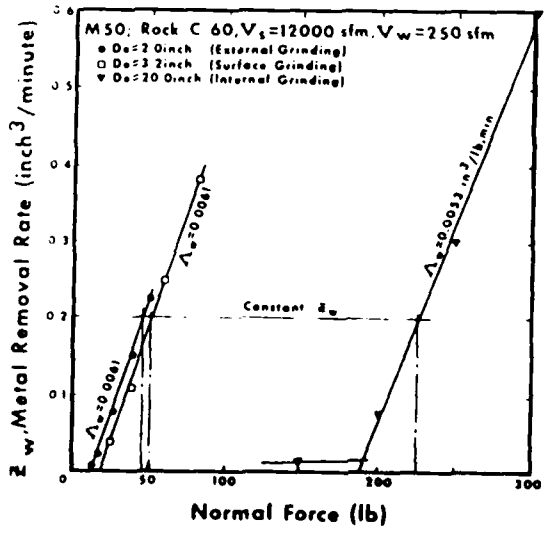
M50; Rock C 60, V_s=12000 sfm, V_w=250 sfm
De=2.0inch (External Grinding)
De=3.2inch (Surface Grinding)
De=20.0inch (Internal Grinding)
Λ_w=0.0061
Λ_w=0.0061
Λ_w=0.00053 in³/lb.min
Constant d_w
Z_w, Metal Removal Rate (inch³/minute)
Normal Force (lb)
0
0.1
0.2
0.3
0.4
0.5
0.6
50
100
200
300

FIG. 19

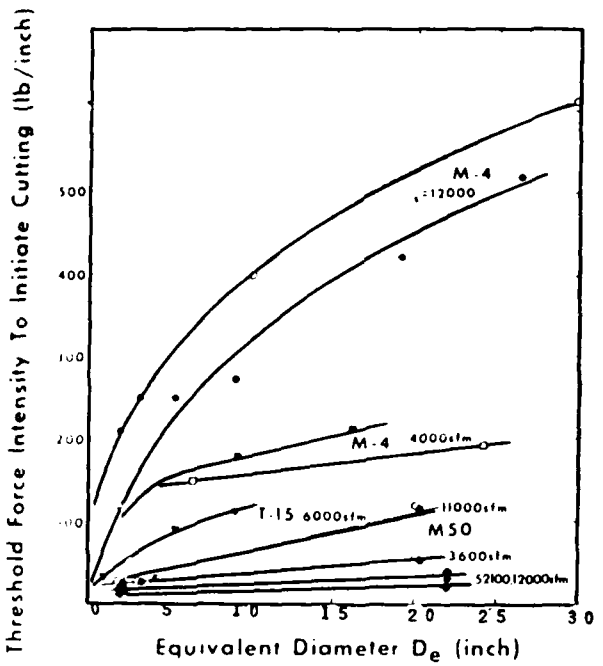
Threshold Force Intensity To Initiate Cutting (lb/inch)
500
400
100
200
M-4
=12000
M-4 4000sfm
T-15 6000sfm
11000sfm
M50
3600sfm
5210012000sfm
0
5
10
15
20
25
30
Equivalent Diameter D_e (inch)

FIG. 20

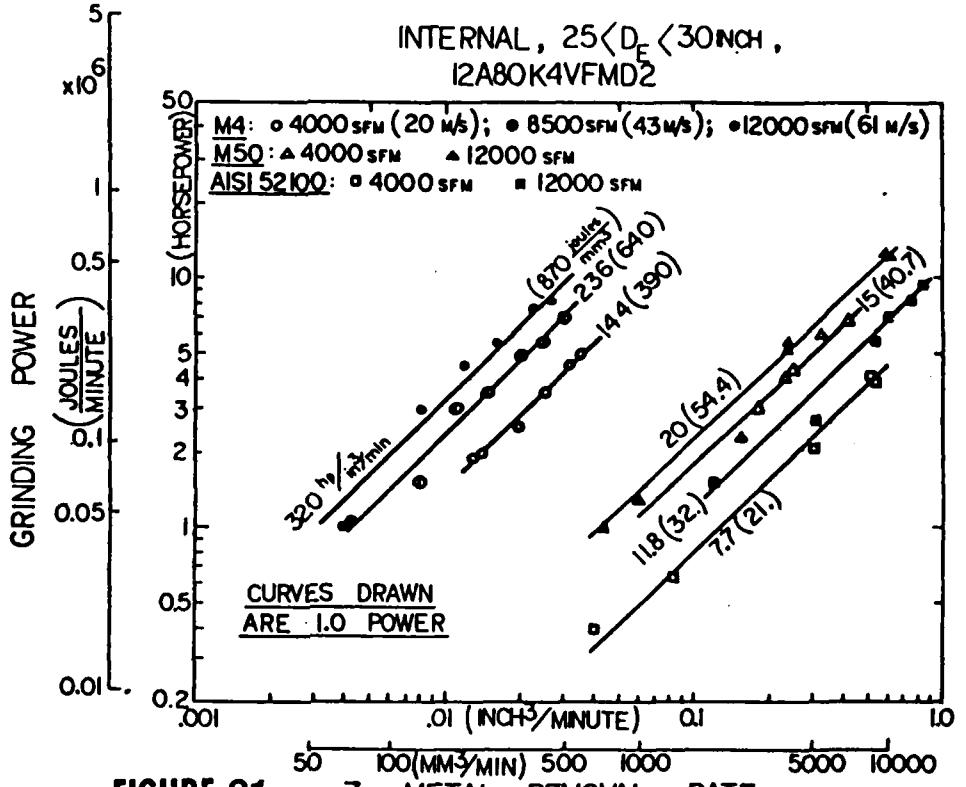

FIGURE 21 Z_W METAL REMOVAL RATE

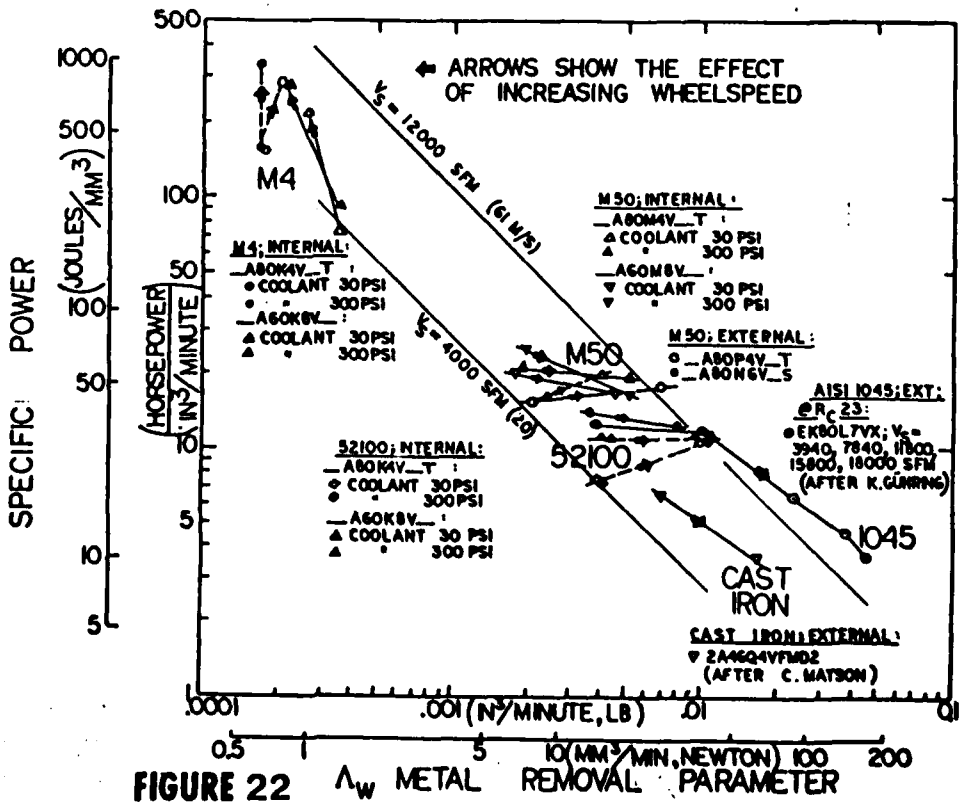

FIGURE 22 Λ_W METAL REMOVAL PARAMETER

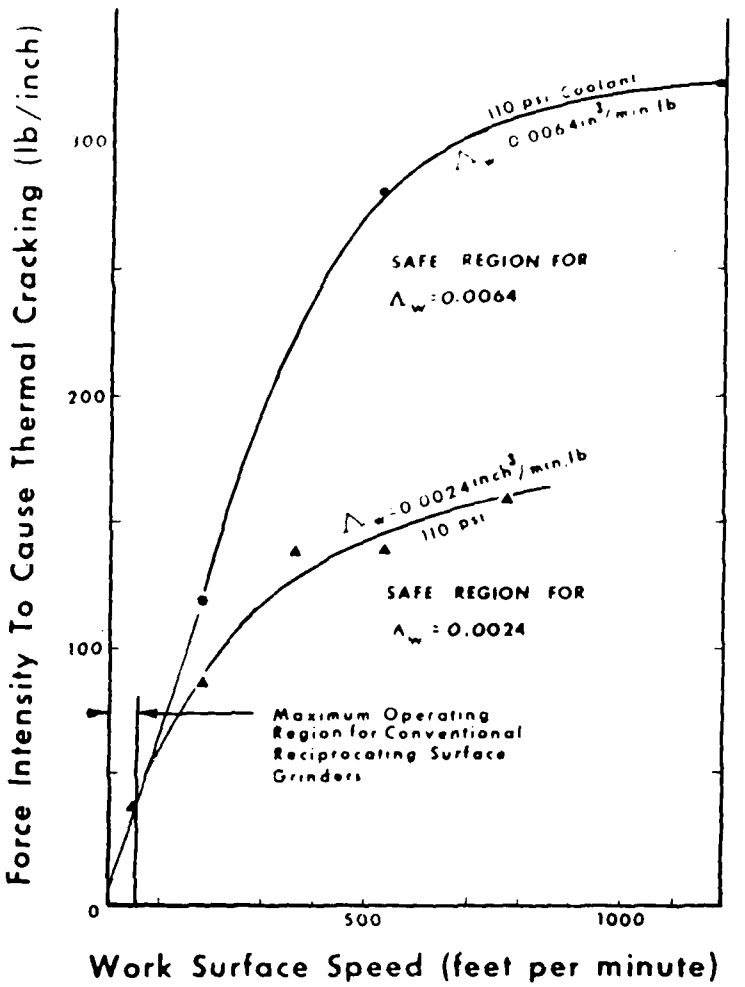
Force Intensity To Cause Thermal Cracking (lb/inch)
300
200
100
0
500
1000
Work Surface Speed (feet per minute)
110 psi Coolant
Λ_w = 0.0064 inch³/min.lb
SAFE REGION FOR
Λ_w = 0.0064
Λ_w = 0.0024 inch³/min.lb
110 psi
SAFE REGION FOR
Λ_w = 0.0024
Maximum Operating Region for Conventional Reciprocating Surface Grinders

FIG. 23

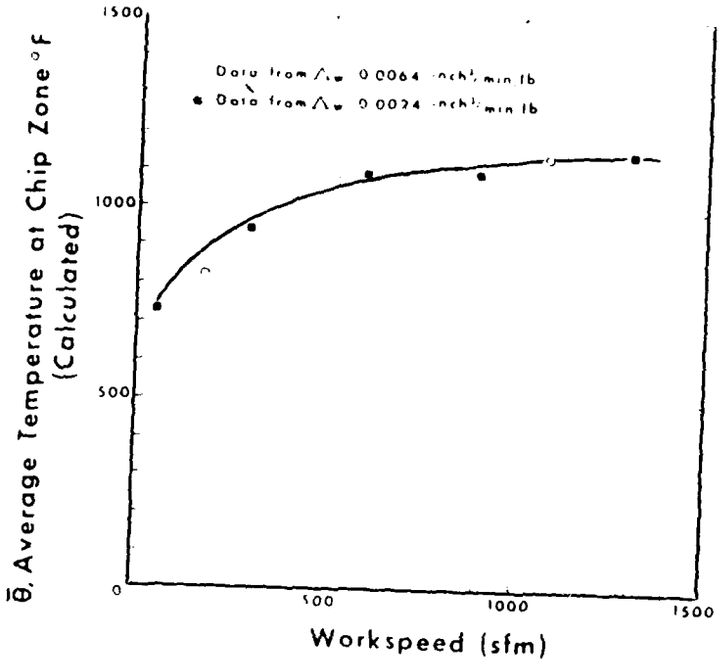
1500
1000
500
0
500
1000
1500
θ̄, Average Temperature at Chip Zone °F (Calculated)
Workspeed (sfm)

FIG. 24

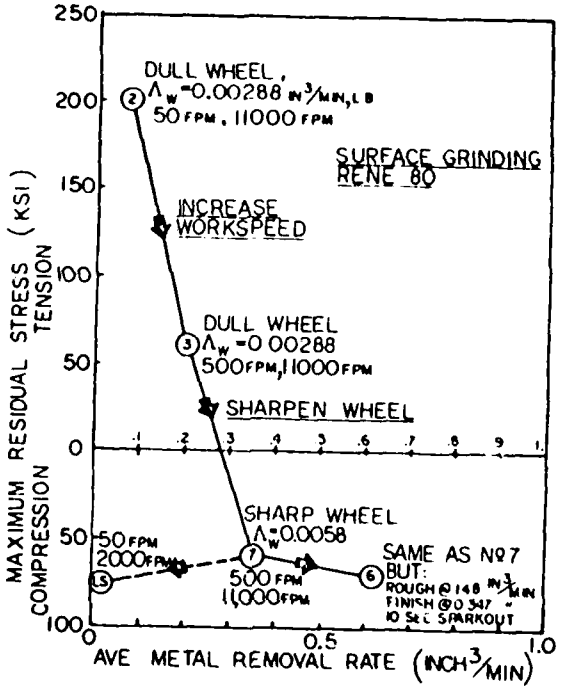
250
200
150
100
50
0
50
100
MAXIMUM RESIDUAL STRESS (KSI)
TENSION
COMPRESSION
DULL WHEEL,
Λ_w=0.00288 IN³/MIN, LB
50 FPM, 11000 FPM
SURFACE GRINDING
RENE 80
INCREASE
WORKSPEED
DULL WHEEL
Λ_w=0.00288
500FPM, 11000FPM
SHARPEN WHEEL
SHARP WHEEL
Λ_w=0.0058
50 FPM
2000FPM
500 FPM
11,000FPM
SAME AS Nº7
BUT:
ROUGH @ 1.48 IN³/MIN
FINISH @ 0.547 "
10 SEC SPARKOUT
0
0.5
1.0
AVE METAL REMOVAL RATE (INCH³/MIN)

FIG. 25

The threshold force intensities to cause incipient cracking of AISI 52100 steel after an acid etch when grinding at normal work speeds are plotted against work speed in Fig. 23 (6) for a dull wheel (WRP = .1 cumm/sec*N the lower curve) and for a sharp wheel (WRP = .335 cumm/sec*N upper curve). It will be seen that high work speeds and sharp wheels permit higher force intensities and stock-removal rates to be used. When the grinding zone temperature is calculated (3), the two curves in Fig. 23 are reduced to a single function as shown in Fig. 24 showing that temperature is the controlling factor.

Good surface integrity can be obtained by operating at high work speeds, using sharp wheels, and not permitting the induced force intensity to exceed some experimentally determined threshold value. Fig. 25 illustrates the effect of increasing work speed and wheel sharpness on residual stress (6). Point 2 corresponds to a dull wheel (WRP = .00288 cu.in/min*lb) and a low work speed (V_w = 50 fpm) resulting in 200,000 lb/sq.in. tensile stress. Point 3 shows the effects of increasing the work speed with the dull wheel. Point 7 corresponds to a sharp wheel (WRP = .0058 cu.in/min*lb) and high work speed, resulting in a residual compressive stress. Methods have recently been developed for automatically monitoring wheel sharpness and induced force intensity to accomplish "Controlled Surface Integrity Grinding". These methods involve force sensors and computer control (12).

5.0 Creep-Feed Grinding

The procedure of setting the wheel to take the full depth-of-cut, and feeding the work slowly under the wheel is known as "Creep-Feed" grinding. It has been found, in a number of surface grinding applications, that stock-removal rates may be two to three times greater than conventional rates, and wheelwear rates are greatly reduced at the same time. This makes the process attractive where forms and profiles must be produced. However, the tendency to burn and thermally damage the workpiece is greatly increased so that the coolant application becomes critical as well as maintaining a sharp wheel.

5.1 Forces in Creep-Feed Grinding

Figure 16 illustrates a grinding wheel taking a deep creep-feed cut. The normal and tangential stress σ_n and σ_t are shown at the position θ. Analogous to Eq. 13 is the following basic stock-removal equation:

$$Z''_w = \Lambda_w \quad (\sigma_n - \sigma_{th}) \tag{31}$$

where Z''_w is the volumetric stock-removal rate per unit area, and σ_{th} is the threshold normal stress.

Since:

$$Z''_w = V_w \sin \theta \tag{32}$$

the normal stress from Eq. 31 is:

$$\sigma_n = \frac{V_w \sin\theta}{\Lambda_w} + \sigma_{th} \tag{33}$$

Also:

$$\sigma_t = \mu\sigma_n \tag{34}$$

where μ is the effective coefficient of friction. Then, an element of the normal force is:

$$dF_n = \sigma_n \, w \, \frac{D_s}{2} \, d\theta \tag{35}$$

$$dF_n = \frac{wD_s}{2}\left[\frac{V_w \sin\theta}{\Lambda_w} + \sigma_{th}\right] d\theta \qquad (36)$$

and the tangential force:

$$dF_t = \mu\sigma_n \frac{wD_s}{2} d\theta \qquad (37)$$

$$dF_t = \frac{\mu wD_s}{2}\left[\frac{V_w \sin\theta}{\Lambda_w} + \sigma_{th}\right] d\theta \qquad (38)$$

The vertical and horizontal forces F_y and F_x are found by integrating:

$$dF_y = dF_n \cos\theta \pm dF_t \sin\theta \qquad (39)$$

$$dF_x = dF_n \sin\theta \pm dF_t \cos\theta \qquad (40)$$

between the limits $\theta = 0$ and $\theta = \theta_o$ where:

$$\theta_o = \cos^{-1}\left(1 - \frac{2h}{D_s}\right) \qquad (41)$$

and,

\+ is used for climb grinding and

\- for conventional grinding.

The results are:

$$F_y = \frac{wD_s}{2}\left[\frac{V_w}{\Lambda_w}\frac{\sin^2\theta_o}{2} + \sigma_{th}\sin\theta_o\right] \pm \frac{\mu wD_s}{2}\left[\frac{V_w}{\Lambda_w}\left(\frac{\theta_o}{2} - \frac{\sin\theta_o\cos\theta_o}{2}\right) - \sigma_{th}(\cos\theta_o - 1)\right] \qquad (42)$$

$$F_x = \frac{wD_s}{2}\left[\frac{V_w}{2\Lambda_w}(\theta_o - \sin\theta_o\cos\theta_o) + \sigma_{th}(1 - \cos\theta_o)\right] \pm \frac{\mu wD_s}{2}\left[\frac{V_w \sin^2\theta_o}{2\Lambda_w} + \sigma_{th}\sin\theta_o\right] \qquad (43)$$

Also, the torque on the wheel is:

$$dT = \frac{D_s}{2} dF_t \qquad (44)$$

$$T = \mu\left(\frac{D_s}{2}\right)^2 w \int_0^{\theta_o} \left[\frac{V_w \sin\theta}{\Lambda_w} + \sigma_{th}\right] d\theta$$

$$= \frac{\mu D_s^2 w}{4} \left[\frac{V_w(1-\cos\theta_o)}{\Lambda_w} + \sigma_{th}\theta_o\right] \qquad (45)$$

These equations may be simplified where the wheel depth-of-cut h is small compared to the wheel radius, thus:

$$\cos\theta_o = 1 - \frac{2h}{D_s}$$

$$1 - \frac{\theta_o^2}{2!} + \text{---} = 1 - \frac{2h}{D_s}$$

$$\theta_o = 2\sqrt{\frac{h}{D_s}} \quad \text{and} \quad \sin\theta_o = \theta_c \qquad (46)$$

Equation 42 simplifies to:

$$F_y = wD_s \left[\frac{V_w h}{\Lambda_w D_s} + \sigma_{th}\sqrt{\frac{h}{D_s}}\right] \qquad (47)$$

For grinding conditions where the threshold stress is negligible, the second term can be dropped giving:

$$F_y = \frac{wV_w}{\Lambda_w} h \qquad (48)$$

so that the cutting stiffness is:

$$K_c = \frac{wV_w}{\Lambda_w} \qquad (49)$$

in agreement with Eq. 22.

5.2 Stock-Removal Rate vs Work Speed

In conventional cylindrical grinding the stock-removal rate is essentially independent of work speed. In Creep-Feed grinding the stock-removal rate is directly proportional to work speed. Thus, two regions exist as shown in Fig. 26(1). The requirements for operating in the Creep-Feed region are outlined below.

Equation 48 gives the separating force F_y when threshold stresses are negligible. This force must be in equilibrium with the elastic force generated by the deflection x of the machine, thus:

$$K_m x = K_c h \tag{50}$$

Also, from Fig. 16:

$$d = h + x \tag{51}$$

Eliminating x gives:

$$h = \frac{K_m}{K_m + K_c} d \tag{52}$$

The stock-removal rate per unit width Z'_w is:

$$Z'_w = \Lambda V_w \tag{53}$$

$$Z'_w = \frac{K_m V_w d}{K_m + K_c} \tag{54}$$

Recalling from Eq. 49 that the cutting stiffness K_c is proportional to work speed, two cases arise:

1. K_c is large compared to K_m
   Equation 54 becomes:
   $$Z'_w = \frac{V_w K_m d}{K_c} = \Lambda_w \frac{K_m d}{w} \tag{55}$$

2. K_c is small compared to K_m.
   Equation 54 becomes:
   $$Z'_w = V_w d \tag{56}$$
   showing that the stock-removal rate is proportional to work speed.

The criterion for operating in the creep-feed region is:

$$K_m \geq 10\ K_c \qquad (57)$$

Therefore, Creep-Feed grinders are designed to withstand large forces and have a large stiffness.

5.3 Work Removal Parameters--Creep Grinding

The general literature on Creep Grinding describes, mostly, production rates and applications. Very little literature exists relating forces and stock-removal rates. However, Salje (10) has reported increasing force levels and reduced wheelwear at very low work speeds. Figure 27 shows the normal force intensity F_n' and the wheelwear experienced at various work speeds and depths-of-cut. The tests were made at a constant stock-removal rate Z_w'. From this figure it will be seen that force intensities tend to rise at very low speeds. Pratt (8) has also reported increased power at very low work speeds. If it is assumed that the friction coefficient between wheel and work μ is .5, then the power readings can be converted into normal force intensity as shown in Fig. 28.

The reason these two investigators have found higher forces and power at very low work speed is related to the excessively large value of D_e (Equivalent Diameter) existing at these conditions. It will be recalled from section 4.3 that the difference in curvature, or D_e, affects the grinding parameters WRP and F_{th}. Equation 11 for the difference in curvature can be simplified to:

$$\Delta_i = \frac{2}{D_s}\left[\frac{\left(1 - \frac{D_s}{D_w}\right)\left(1 + 2S\right)}{(1 + S)^2}\right] \qquad (58)$$

where S = Wheel Surface Speed/Work Surface Speed. For surface grinding $D_w \to \infty$ and Eq. 58 becomes:

$$\Delta_i = \frac{2}{D_s}\left[\frac{1 + 2S}{(1 + S)^2}\right] \qquad (59)$$

or:

$$D_e = \frac{2}{\Delta_i} = \frac{(1 + S)^2}{1 + 2S} D_s \qquad (60)$$

The values of D_e are also plotted in Fig. 28 for Pratt's power data. It will be seen that the power increases as the value of D_e becomes excessively large, then drops down again. This indicates there is some value of work speed where power and forces

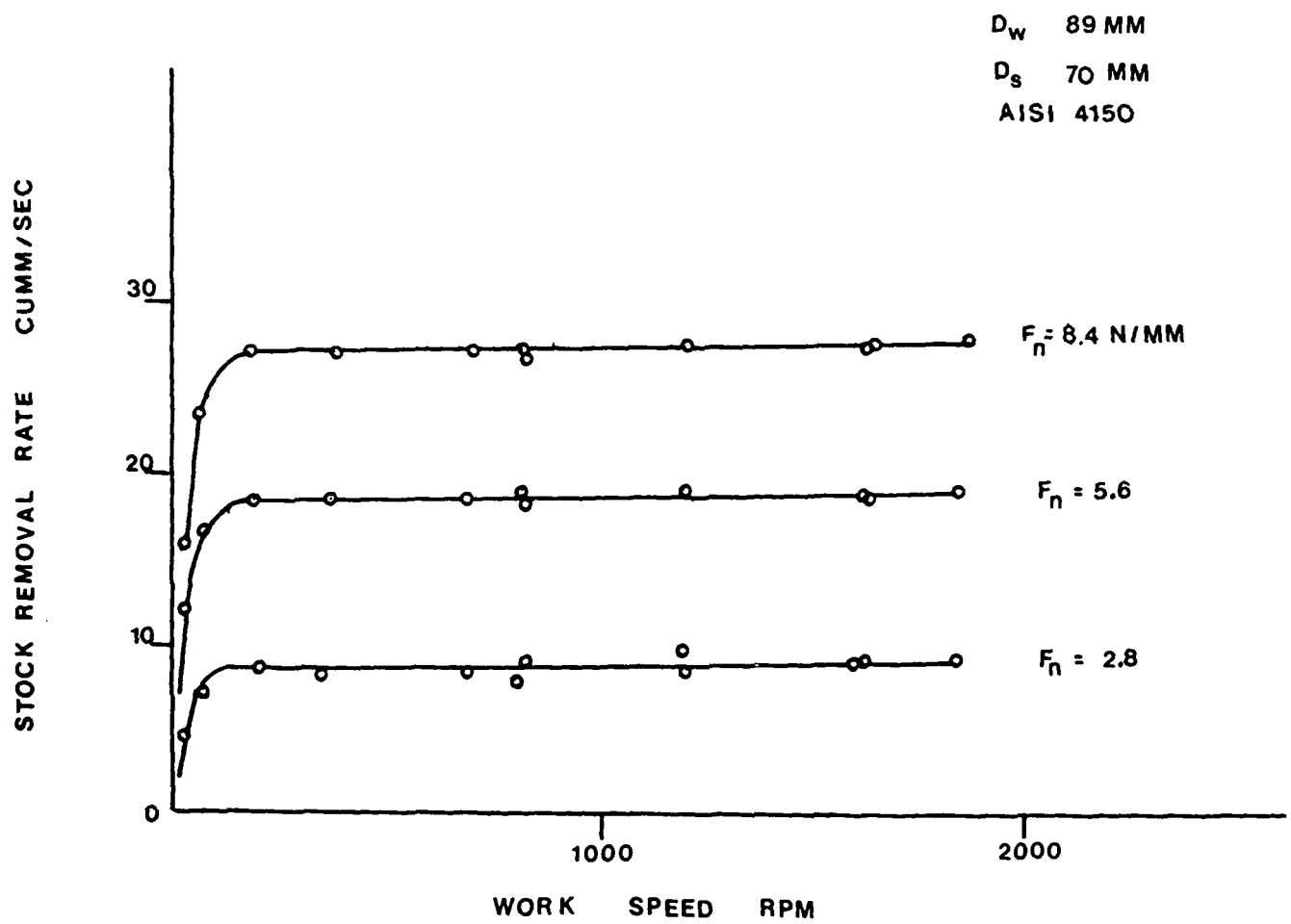
D_w 89 MM
D_s 70 MM
AISI 4150
STOCK REMOVAL RATE CUMM/SEC
30
20
10
0
F_n = 8.4 N/MM
F_n = 5.6
F_n = 2.8
1000
2000
WORK SPEED RPM

FIG 26

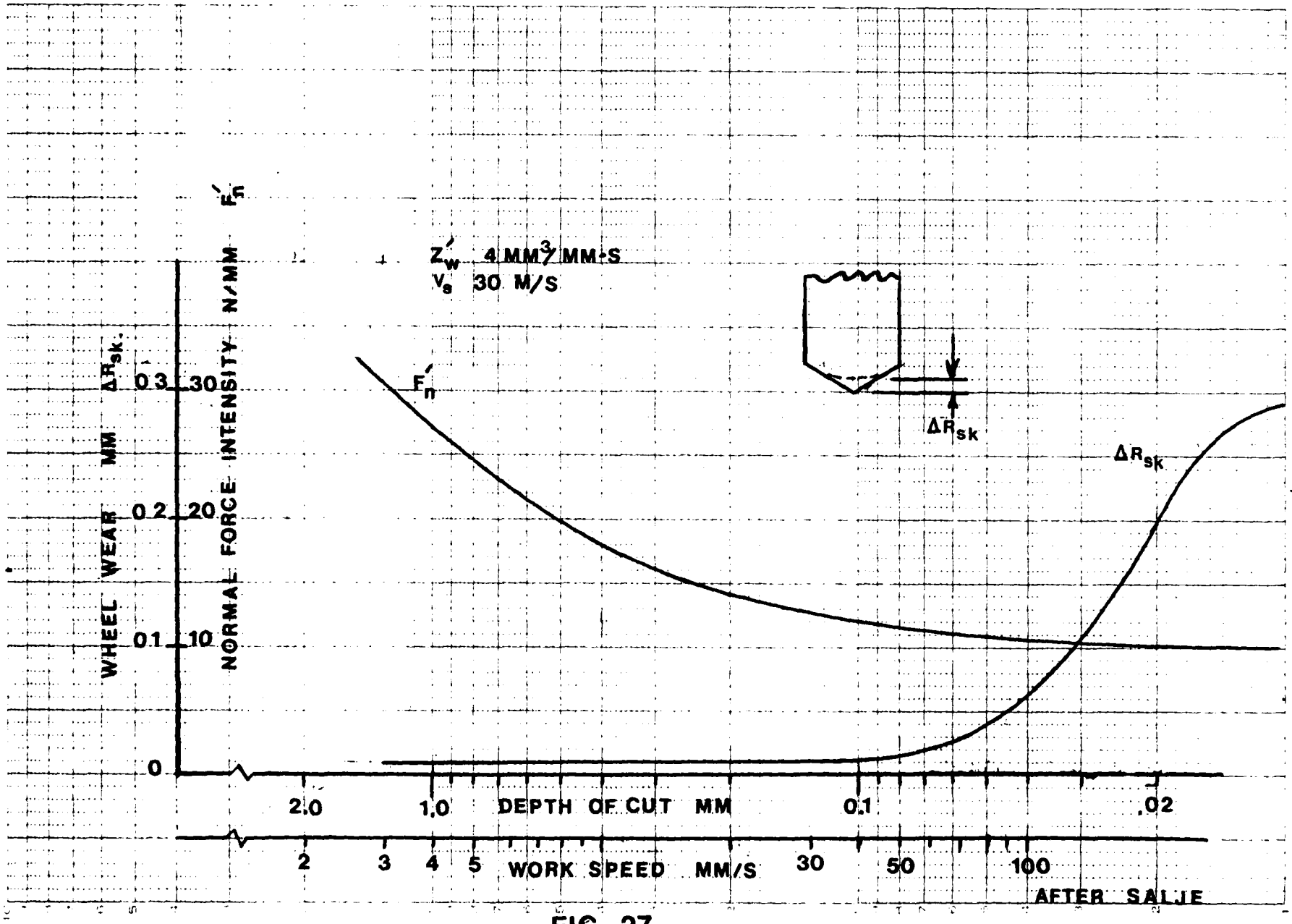
Z'_w 4 MM^3/MM-S
V_s 30 M/S
F'_n
ΔR_{sk}
ΔR_{sk}
WHEEL WEAR MM ΔR_{sk}.
NORMAL FORCE INTENSITY N/MM F'_n
0.3
0.2
0.1
0
30
20
10
2.0
1.0
DEPTH OF CUT MM
0.1
.02
2
3
4
5
WORK SPEED MM/S
30
50
100
AFTER SALJE

FIG 27

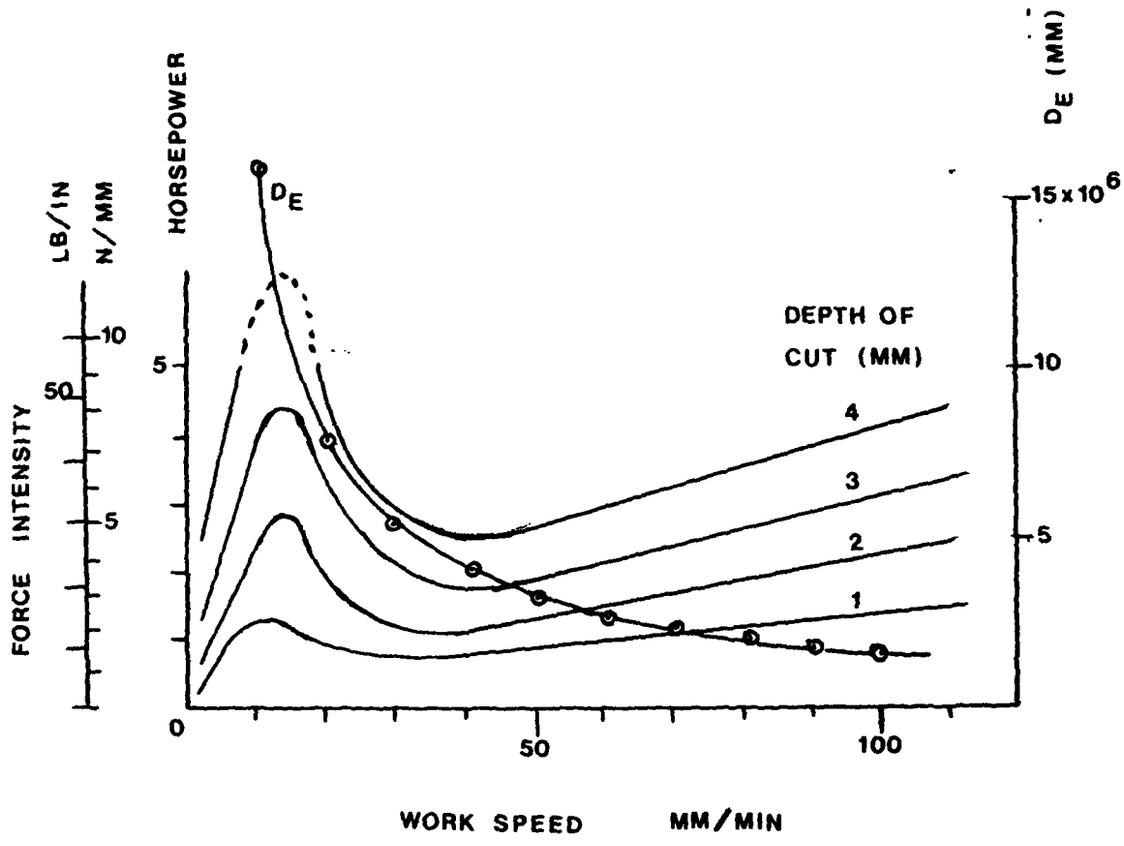
FORCE INTENSITY
LB/IN
N/MM
HORSEPOWER
D_E
D_E (MM)
15×10^6
DEPTH OF
CUT (MM)
10
50
5
0
50
100
4
3
2
1
WORK SPEED MM/MIN

FIG 28

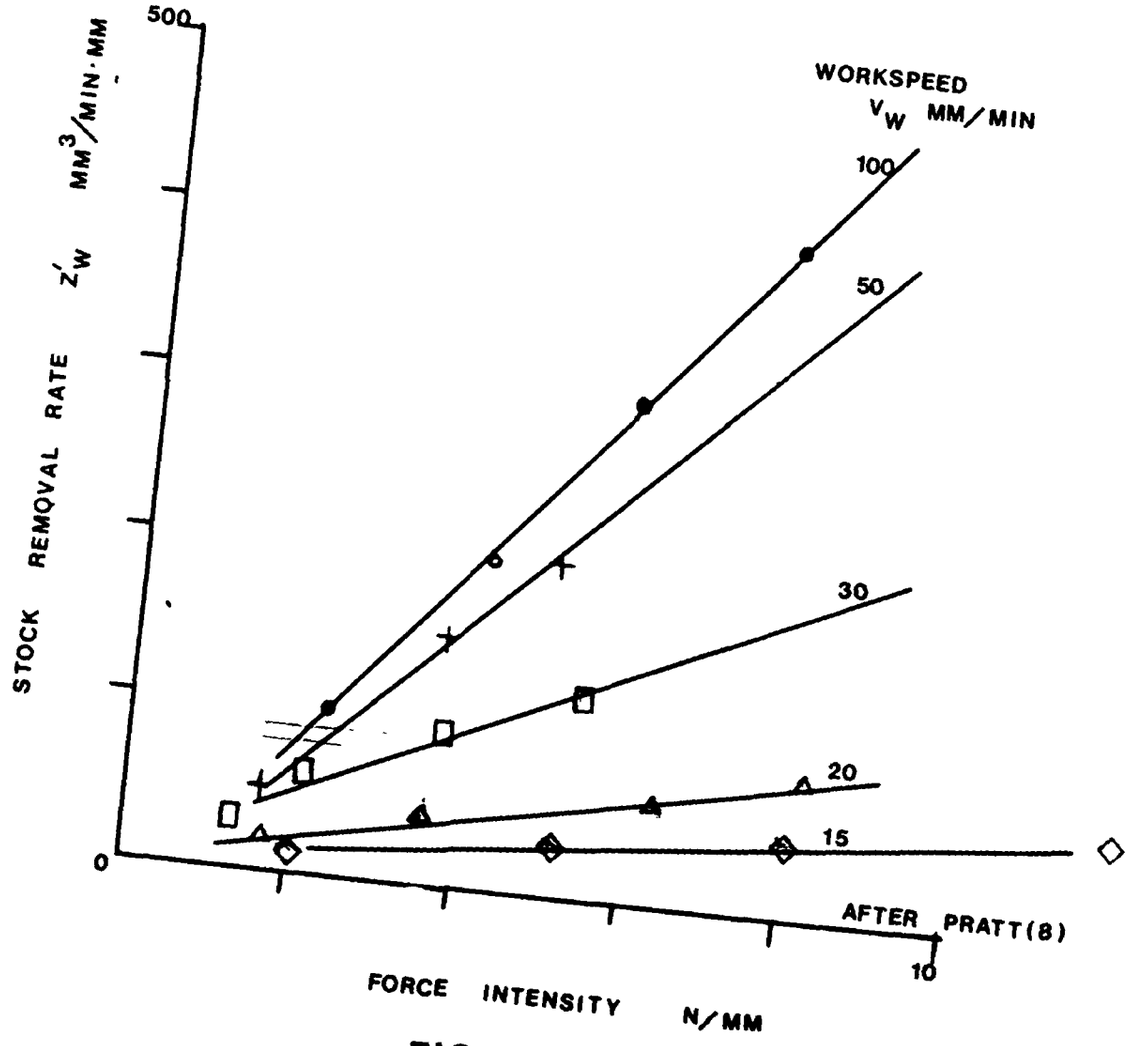
500
0
STOCK REMOVAL RATE z'_w $MM^3/MIN \cdot MM$
WORKSPEED
V_W MM/MIN
100
50
30
20
15
AFTER PRATT(8)
10
FORCE INTENSITY N/MM

FIG 29

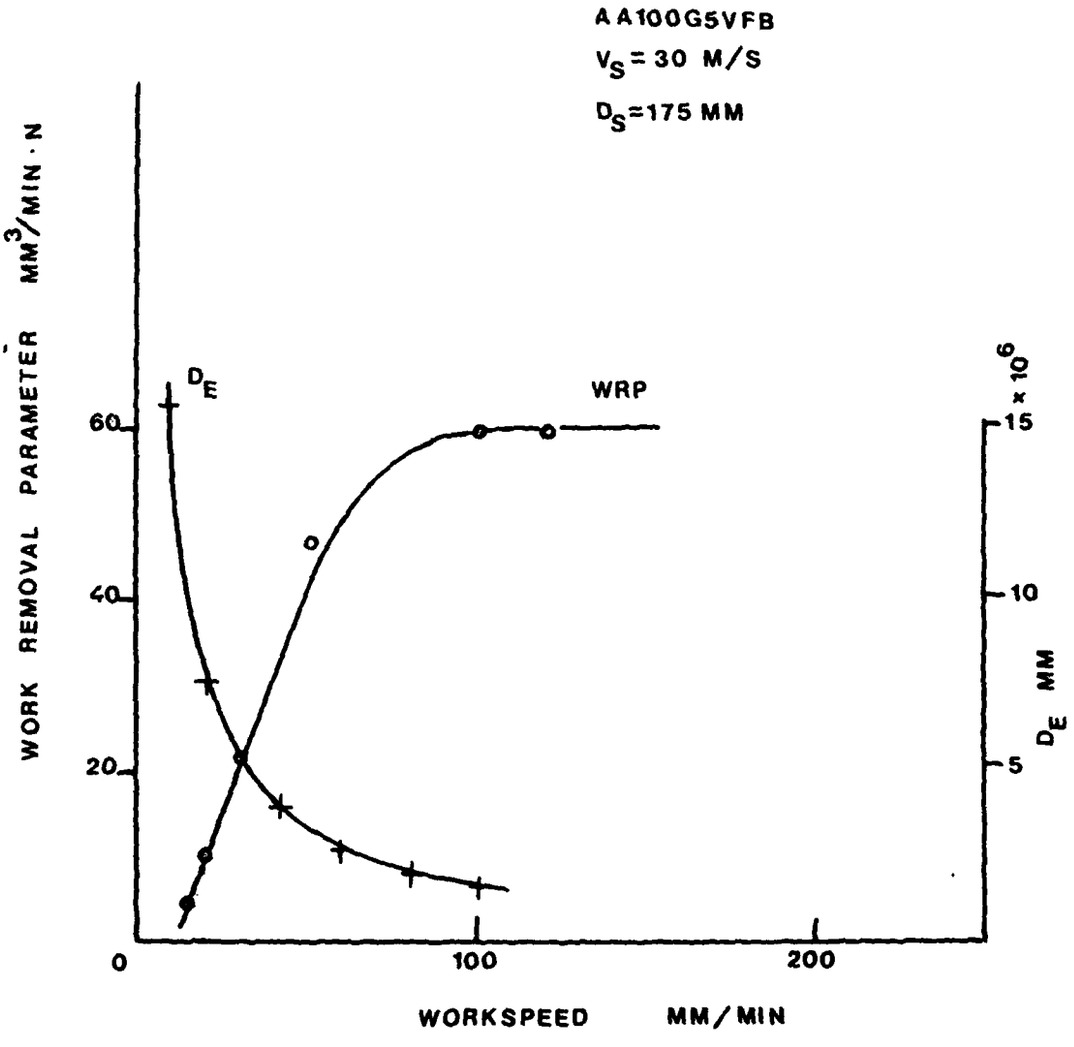
AA100G5VFB
V_S = 30 M/S
D_S=175 MM
WORK REMOVAL PARAMETER MM³/MIN·N
D_E
WRP
60
40
20
0
100
200
15
10
5
$\times 10^6$
D_E MM
WORKSPEED MM/MIN

FIG 30

are a minimum. Using the data of Fig. 28, the stock-removal rate Z'_w can be plotted aginst normal force intensity as shown in Fig. 29 for several values of work speed or D_e. The slope of these curves is the Work Removal Parameter Λ_w. It will be seen that the Work Removal Parameter drops rapidly as the Equivalent Diameter becomes excessively large. Figure 30 shows the WRP and the D_e plotted directly against work speed. In grinding the K9 Tool Steel used by Pratt, the D_e should not be allowed to exceed 2000 meters. Some typical values of Creep Feed grinding parameters are given in Table 6.

5.4 Grind Time--Normal Work Speed vs Creep

In addition to combining operations as suggested in section 3.0, reducing the grind time for each operation obviously improves productivity and reduces grinding costs. The grind time for executing the ID grind (operation 50ID and 60) on the Vane-Cluster Assembly shown in Figures 6 and 9 will be estimated for both Creep Feed and normal work speed grinding.

In normal work speed grinding, the wheel is fed into the workpiece at the rough-grind feedrate. The extreme tip of the wheel for grinding the deep groove will strike the workpiece first and only after some time has passed will the wheel become fully engaged with the workpiece. Using Eq. 15 and a typical value for the Work Removal Parameter Λ_w of .0045 $in^3/min.lb$ ($16mm^3/min \cdot N$) gives the feedrate to produce a normal force intensity of 167 lb/in.

$$\bar{v}_w = \frac{\Lambda_w F_n}{\pi D_w W} = \frac{.0045 \times 200}{\pi 42 \times 1.20} = .0057 \text{ in/min}$$

At this feedrate the time required to remove .360 in. of stock (excluding dressing time) is:

$$\text{Grind Time} = \frac{.360}{.0057} = 63 \text{ min.}$$

and the fully engaged stock-removal rate is:

$$Z'_w = \Lambda_w F'_n = .0045 \times 200/1.2 = .75 \text{ in}^2/\text{min}$$

$$Z_w = Z'_w W = .75 \times 1.2 = .90 \text{ in}^3/\text{min}$$

With the Creep Feed mode of grinding, the wheel is set to full depth (in a gap between two vane clusters), the table is rotated at a creep-feed rate taking the full depth-of-cut in one revolution.

The area of cut A, from Fig. 9 is .124 in.^{2}, and the stock-removal rate is:

$$Z_w = A\ V_w$$

From Eq. 13:

$$Z_w = \Lambda_w\ F_n$$

Therefore:

$$A\ V_w = \Lambda_w\ F_n$$

and the creep-feed rate is:

$$V_w = \frac{\Lambda_w\ F_n}{A} = \frac{.0045 \times 200}{.124} = 7.26 \text{ in/min.}$$

In this case the Creep Feed Grind Time is:

$$\text{Grind Time} = \frac{\pi\ D_w}{V_w} = \frac{\pi\ 42}{7.26} = 18.2 \text{ min.}$$

and the full stock-removal rate is achieved as soon as the complete "footprint" (Fig. 31) is developed. Thus:

$$Z = A\ V_w = .124 \times 7.26 = .90 \text{ in}^3\text{/min.}$$

as before.

From this it can be seen that the creep grinding of forms or profiles is much faster (18 vs 63 min.) because the full stock-removal rate can be developed much sooner than in normal work speed grinding where considerable distance must be fed to completely engage the wheel.

5.5 Wheelwear--Normal Work Speed vs Creep

Another major characteristic of creep-feed grinding is the greatly reduced wheelwear rate. In grinding at normal work speeds, the contact area or "footprint" between wheel and workpiece is relatively small, and the unit pressure relatively high. In creep-feed grinding the contact area is much larger, and the unit pressure relatively low. This results in greatly reduced wheelwear. Salje (10) found a 29 to 1 drop in wheelwear as shown in Fig. 27 as work speed was reduced while maintaining the same stock-removal rate Z'_w. The experience of others (7,8,9, 11) generally confirms this observation.

In order to relate wheelwear under a wide variety of conditions it is convenient to use the volumetric rate of wheelwear per unit width of cut Z'_s, divided by the wheel surface speed V_s. This quantity, Z'_s/V_s, represents the thickness of the extremely thin layer of abrasive material being worn away from the surface of the wheel each revolution.

Extensive measurements of wheelwear under carefully controlled conditions have been carried out by Lindsay (5) for internal, external and rotary surface grinding at normal work speeds. Figures 32, 33, 34 show the wear thickness Z'_s/V_s, plotted against average normal contact pressure with the corresponding operating data given in Tables 7, 8, 9. From these data the wear thickness is found to obey:

$$\frac{Z'_s}{V_s} = WP \times D_e \, P^3 \quad (in) \tag{61}$$

where: $WP = .407 \times 10^{-17}$ the Wear Parameter

D_e is the Equivalent Diameter (in)

P is the average normal pressure (psi)

In order to use this equation it is necessary to know the length of the contact area l_c (in), between wheel and work. For grinding at normal work speeds (2):

$$l_c = \frac{.214(D_e F'_n)^{\frac{1}{3}}}{44.6 - vol} + \left[\frac{(F'_n - F'_{th})\Lambda_w D_e}{V_w}\right]^{\frac{1}{2}} \tag{62}$$

where: $vol = 1.33H + 2.2S - 8$ (63)

H = 0,1,2,3 ... for H,I,J,K...wheel hardness

S = wheel structure number.

The first term in Eq. 62 is due to the elastic deformation of the wheel in the contact region, and the second term is due to the depth-of-cut. For creep-feed grinding:

$$l_c = \frac{.214\ (D_e F'_n)^{\frac{1}{3}}}{44.6 - vol} + (hD_s)^{.5} \tag{64}$$

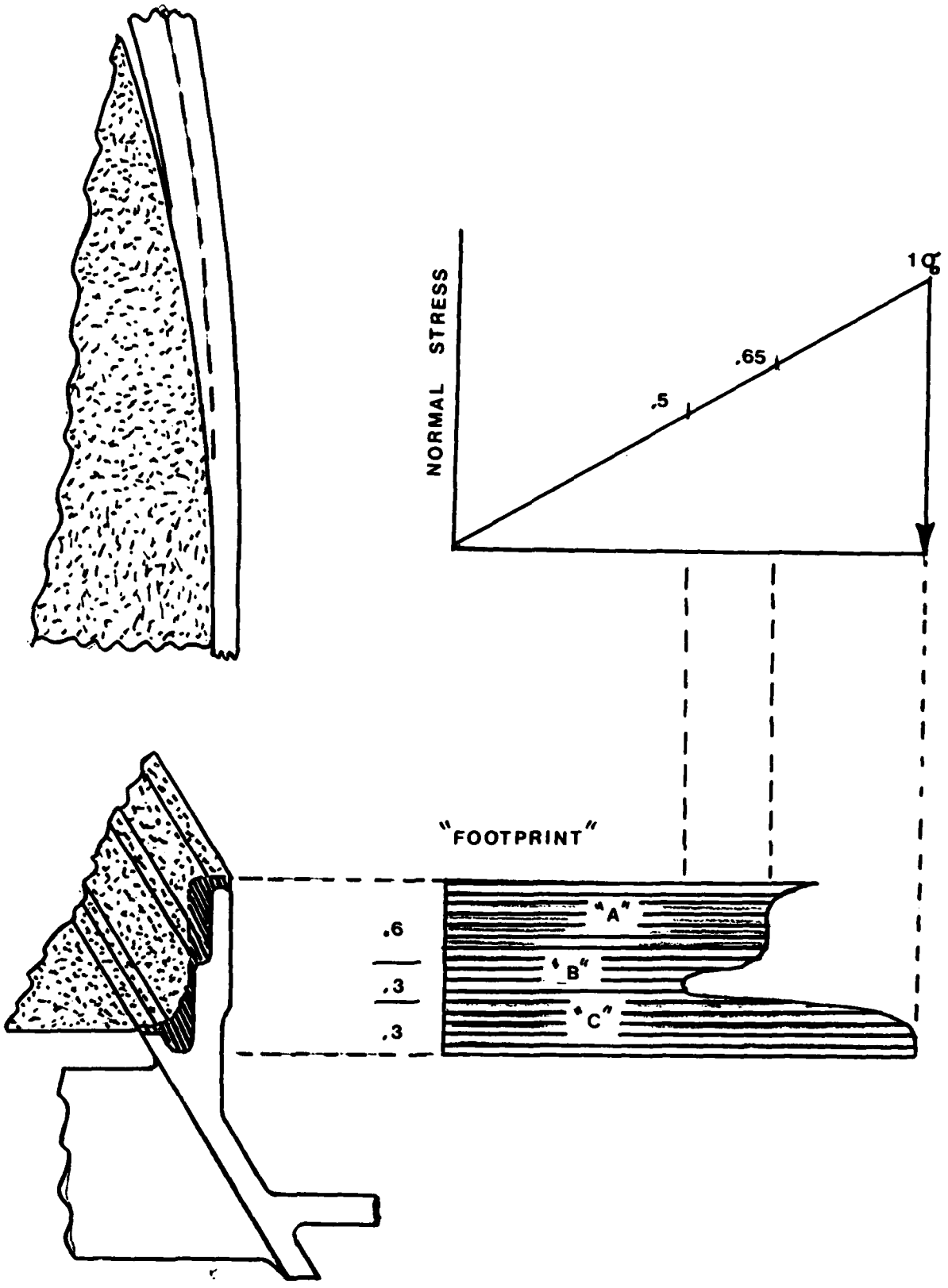

FIG 31

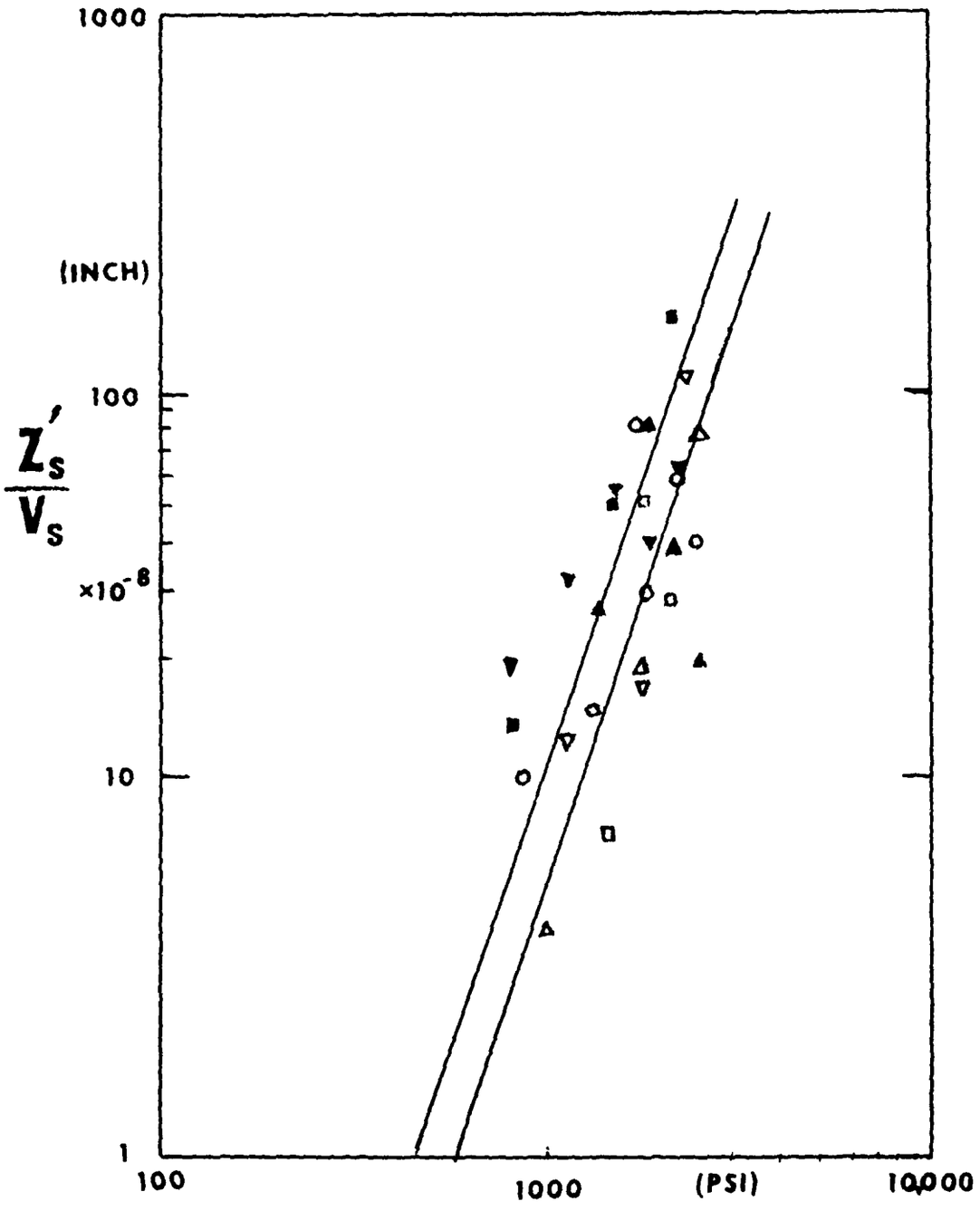

GROSS CONTACT PRESSURE

FIGURE 32

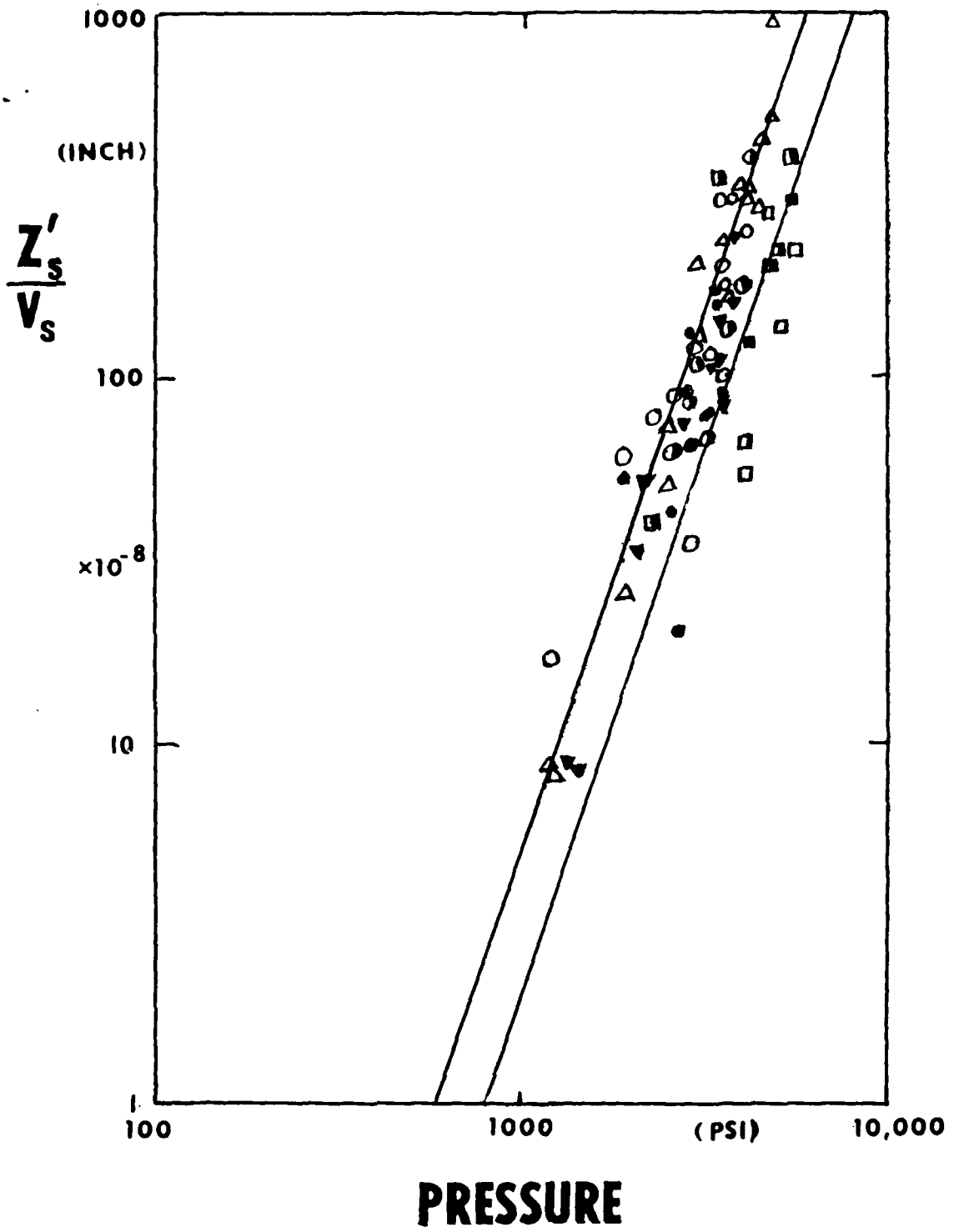
1000
(INCH)
$\frac{Z'_s}{V_s}$
100
$\times 10^{-8}$
10
1
100
1000
(PSI)
10,000
PRESSURE

FIGURE 33

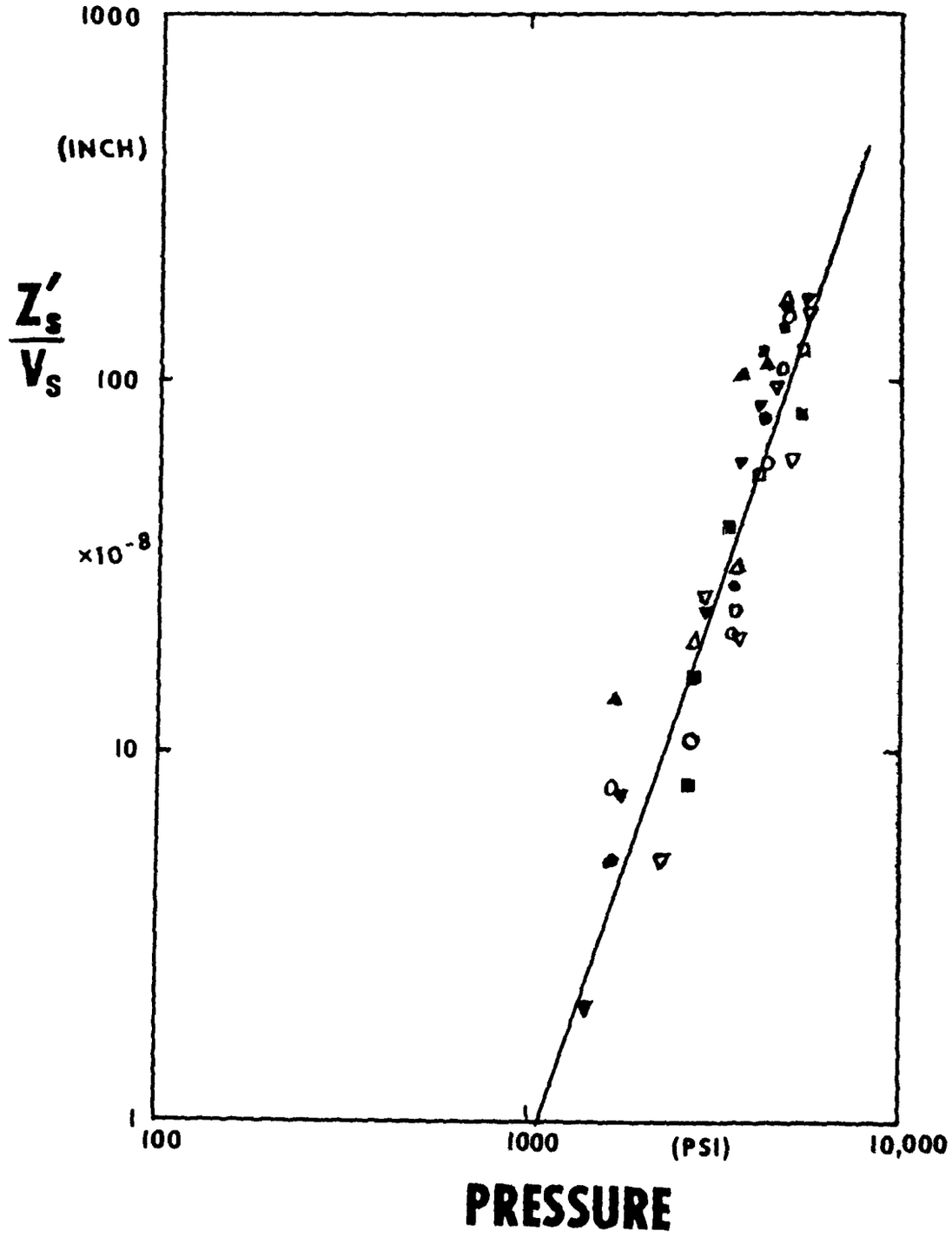
1000
(INCH)
$\frac{Z'_s}{V_s}$
100
$\times 10^{-8}$
10
1
100
1000
(PSI)
10,000
PRESSURE

FIGURE 34

In grinding the vane cluster in Fig. 31 at normal work speeds with Λ_w = .0045 in^3/min.lb, and F_n = 200 lb, the length of contact, from Eq. 62, may be found. Calculating first the value of D_e in the X direction from Eq. 9 for a 60^0 inclination angle gives:

$$XD_e = \frac{D_w D_s/\cos 60}{D_w - D_s/\cos 60}$$

$$= \frac{42 \times 14/.5}{42 - 14/.5} = 84 \text{ in.}$$

The wheel hardness term "vol" for a K grade, 5 structure wheel from Eq. 63 is:

$$\text{vol} = 1.33 \times 3 + 2.2 \times 5 - 8 = 7.0$$

The length of contact at 15 rpm work speed from Eq. 62 is:

$$l_c = \frac{.214(84 \times 167)^{\frac{1}{3}}}{44.6 - 7} + \left(\frac{167 \times .0045 \times 84}{\pi \times 42 \times 15}\right)^{\frac{1}{2}}$$

$$= .137 + .179 = .316 \text{ in.}$$

Then, the average normal contact pressure is:

$$P = \frac{F_n}{A} = \frac{200}{1.2 \times .316} = 527 \text{ psi}$$

From Eq. 61 the wear thickness is:

$$\frac{Z_s'}{V_s} = .407 \times 10^{-17} \times 84\,(527)^3$$

$$= 5.0 \times 10^{-8} \text{ in.}$$

For a 14 in. diameter wheel running at 1750 rpm the wear velocity $\bar{v}_s$ is:

$$\bar{v}_s = \frac{Z_s'}{V_s} N_s = 5.0 \times 10^{-8} \times 1750$$

$$\bar{v}_s = 87.50 \times 10^{-6} \text{ in/min.}$$

This wheelwear rate governs how fast the form or profile on the wheel will be lost. For example, if the groove-cutting portion

of the wheel is required to cut 10 min. before the other areas of the wheel become engaged, it will experience a radial wear of 875 microinches. The wheelwear in creep-feed grinding will be much less as shown below.

For grinding the vane cluster in Fig. 31 in the creep-feed mode, the contact length is much greater as shown in Fig. 31. For example, the length of contact in region "C" from Eq. 64 is:

$$l_c = .137 + (.360 \times 14/\cos 60)^{.5} = 3.31 \text{ in.}$$

The force contributions from the three regions in Fig. 31 are:

$$F_A = (.6 \times 2.3 \times .65/2)\sigma_o = .448\ \sigma_o$$

$$F_B = (.3 \times 1.7 \times .5/2)\sigma_o = .127\ \sigma_o$$

$$F_C = (.3 \times 3.3 \times .5)\sigma_o = .495\ \sigma_o$$

where σ_o is the normal stress at the leading edge of the footprint. Since the total normal force is F_n:

$$F_A + F_B + F_C = F_n$$

$$(.448 + .127 + .495)\sigma_o = 200$$

and the maximum stress is:

$$\sigma_o = \frac{200}{1.07} = 187 \text{ psi}$$

Then, $F_A = 83.8$ lb

$F_B = 23.7$ lb

$F_C = 92.6$ lb

as shown in Fig. 9.

In creep-feed grinding there is no sparkout process as in normal grinding so that the final shape of the part may be distorted due to either part deflection or wheel deflection. Therefore, it is important to consider the work and wheel deflections under the heavy creep-feed forces. It will be appreciated that the deflections will decay as the wheel exits from the cut. This may cause a form error in the workpiece depending upon the stiffness of the system.

Equation 61 may be used to calculate the wear thickness value. The wear parameter WP in Eq. 61 can be determined "on

line" by the computer as follows: After the wheel has been dressed, a selected surface of the wheel is positioned by the computer against the Wheelwear Measuring Station's sensing switch illustrated in Fig. 10. When this switch makes contact the wheel position is saved. The wheel then goes to its grinding position. After grinding for a known time and pressure P, derived from the load cell reading, the computer repositions the wheel at the Wheelwear Measuring Station and feeds it against the switch until contact is again made. The difference in positions gives the actual wheelwear. The wear parameter WP can then be derived.

Using an average value of $.407 \times 10^{-17}$ for the wear parameter and $D_e = 84$ in. Eq. 61 becomes:

$$\frac{Z'_s}{V_s} = 34 \times 10^{-17} P^3$$

Then for region "A", the average pressure and wear rate are:

$$P_A = .65 \times 187 \times .5 = 60.7 \text{ psi}$$

$$\frac{Z'_s}{V_s} = 34 \times 224479. \times 10^{-17} = 76.7 \times 10^{-12} \text{ in.}$$

$$\bar{v}_s = 76.7 \times 10^{-12} \times 1750 = .134 \times 10^{-6} \text{ in/min.}$$

For region "B":

$$P_B = .5 \times 187 \times .5 = 46.7 \text{ psi}$$

$$\frac{Z'_s}{V_s} = 34 \times 102175 \times 10^{-17} = 34.9 \times 10^{-12} \text{ in.}$$

$$\bar{v}_s = 34.9 \times 10^{-12} \times 1750 = .061 \times 10^{-6} \text{ in/min.}$$

For region "C":

$$P_C = 187 \times .5 = 93 \text{ psi}$$

$$\frac{Z'_s}{V_s} = 34 \times 804357 \times 10^{-17} = 275. \times 10^{-12} \text{ in.}$$

$$\bar{v}_s = 275 \times 10^{-12} \times 1750 = .481 \times 10^{-6} \text{ in/min.}$$

From the above it will be seen that the wear rate in region "C" is 87.5/.481 or 182 times smaller when creep-feed grinding as compared to normal grinding. Also, the wear rate in region "C" is about 8 times greater than the wear rate in region "B".

These calculations, when carried out in the computer, permit the computer to estimate differential wheelwear over different sections of the wheel and to prevent the form errors from exceeding the form-error tolerance.

6.0 Control System--Force-Adaptive Grinding

The problem of reducing grinding costs; improving product quality, and operating with personnel having a minimum of grinding expertise, confronts many plants. Grinding operations often produce parts that do not conform precisely to what is desired. Holding precision size, or roundness and concentricity, form or taper or surface finish without burn, in a short cycle time, is often difficult to achieve. These problems arise because of the inability to control certain variables in the grinding process. It is, therefore, important to identify those variables, and to bring them under control to insure consistent size, form, taper, surface finish, and surface integrity (freedom from burn), and product quality.

On conventional grinding machines, the feedrate is controlled. As the grinding wheel engages the workpiece, forces are induced between wheel and work--the higher the force, the faster the stock removal. The induced force also governs the surface finish, the deflection in the machine, the wheelwear rate, and the onset of thermal damage. Therefore, the induced force is one of the important variables which is uncontrolled in conventional feedrate grinding machines.

The ability of the cutting surface of the grinding wheel to remove stock, called the Wheel Sharpness, is the second extremely important variable in the grinding process. In feedrate grinding, as the Wheel Sharpness drops (wheel becomes dull or glazed), the induced force rises resulting in increased deflection and, sometimes, thermal damage.

To obtain consistent grinding results of high quality, and to reduce or eliminate continual operator supervision, it is necessary to control the two important grinding process variables, the interface force and the wheel sharpness as illustrated in Fig. 11. In order to do this, a force sensor is built into the wheelhead which can be calibrated in terms of grinding force, and interfaced to the computer control. Force sensors of the noncontacting type can measure minute deflections of the rotating wheelhead spindle resulting from the grinding force. Once the computer has access to the grinding force, it can manage the grinding cycle to provide improved performance with less operator attention. For example, in grinding the vane cluster shown in Fig. 31, the section "C" of the wheel may wear more than section "B" or "A" producing a form error. The computer, knowing the force intensity F'_n or pressure P, and the wheelwear parameter, can estimate the wheelwear and, in particular,

the differential wheelwear between section "C" and section "A", and can initiate a dressing operation to prevent excessive form errors. Secondly, and of equal importance, the computer, knowing the induced force for a given feedrate can determine the Wheel Sharpness and also initiate a dressing operation when the wheel becomes dull to prevent thermal damage of the workpiece. It can also prevent a build-up of induced force which would otherwise further contribute to thermal damage. In addition, as these forces change, the computer can also compensate for deflections in the system thereby providing more precise sizing of the workpiece. In particular, in creep-feed grinding heavy forces are generated and as the wheel exits from the cut these forces decay and cause a roundness or shape error. The computer, knowing the system stiffness and the cutting stiffness, can compensate for the changing deflection to eliminate these shape errors as explained in detail in Ref. (13).

6.1 Load Cell Wheelhead

Figure 35 shows a standard Whitnon wheelhead Type 411-0032-090 fitted with a pair of noncontacting sensors. The sensors are mounted 180 degrees apart inside the wheelhead, just behind the wheel collet in a horizontal plane to read the normal grinding force. They are interfaced through a printed circuit board in the push-button control box on top of the computer terminal to a Digital PDP11/03 microcomputer. The meter on the control box gives a visual indication of the grinding force. The other push buttons on the box are used for jogging, setup, and operating an XY plotter which simulates a two-axis grinding machine.

The wheelhead was driven by a standard motor, and while running idle, the computer was instructed to read the load cell at closely spaced intervals, and store these readings in memory in order to obtain the "noise level" of the wheelhead and load cell. It will be appreciated that small precessional movements of the spindle axis caused by the bearings will cause voltage fluctuations in the load cell signal, and will appear as "noise" in the system. The stored readings were later retrieved and plotted.

The stiffness of the wheelhead spindle in Fig. 35 was measured and found to be K_m = 333000 lb/in. The load cell system was calibrated by applying known forces at the wheel collet and reading the resulting digital signal. This produced a calibration factor of .117 lb. for an octal unit (least significant bit) in the captured computer word. Figure 36a shows the load cell "noise" plotted in terms of force where the readings were captured every .01 seconds. Figure 36c and 36d are similar plots but with reading intervals of .02 and .05 sec. The wheelhead speed was 1750 rpm except for Fig. 36b where the spindle was at rest.

FIG 35 64.

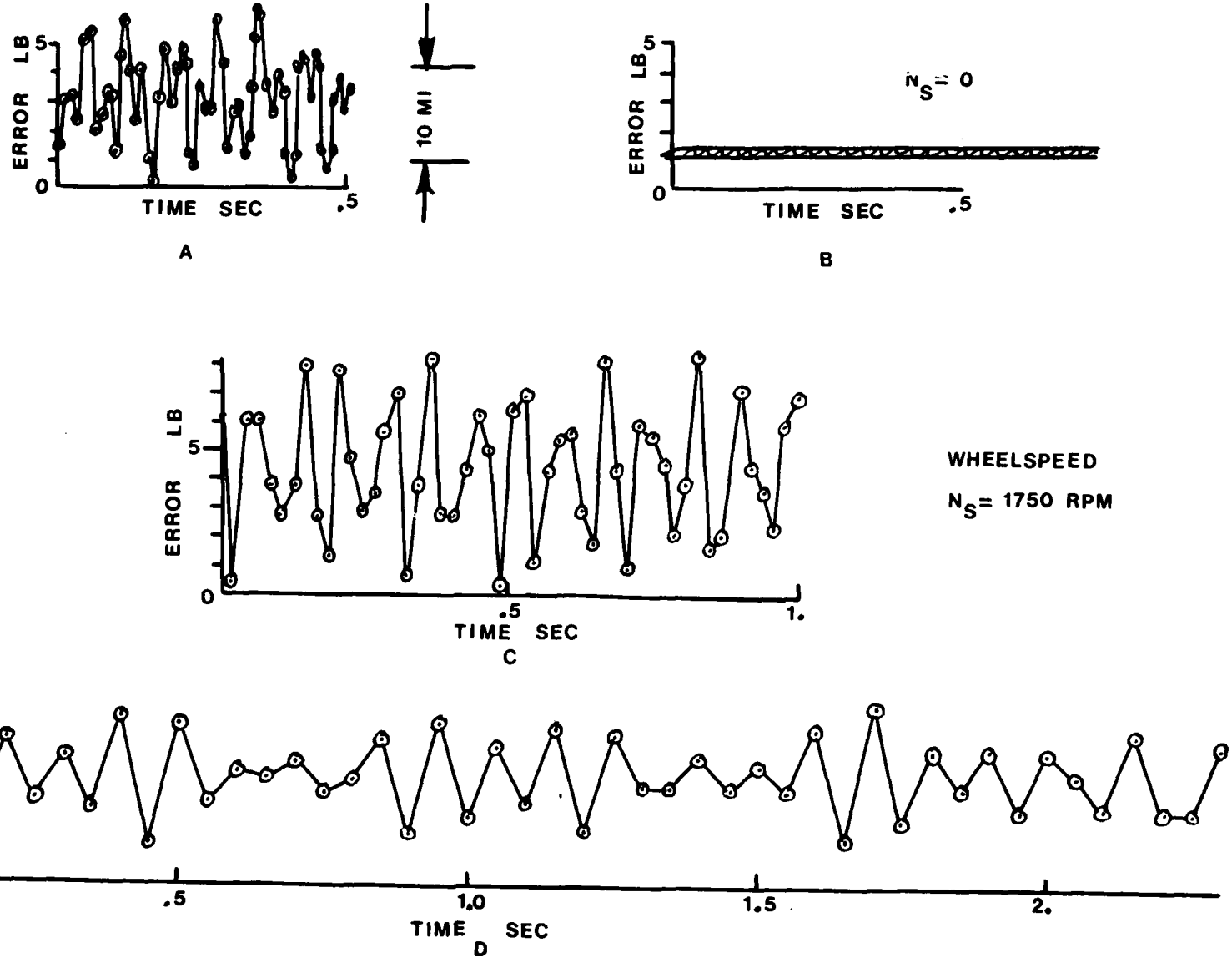
ERROR LB
5
0
TIME SEC
.5
A
10 MI
ERROR LB
5
0
$N_S = 0$
TIME SEC
.5
B
ERROR LB
5
0
.5
1.
TIME SEC
C
WHEELSPEED
N_S= 1750 RPM
ERROR LB
5
0
.5
1.0
1.5
2.
TIME SEC
D

FIG 36

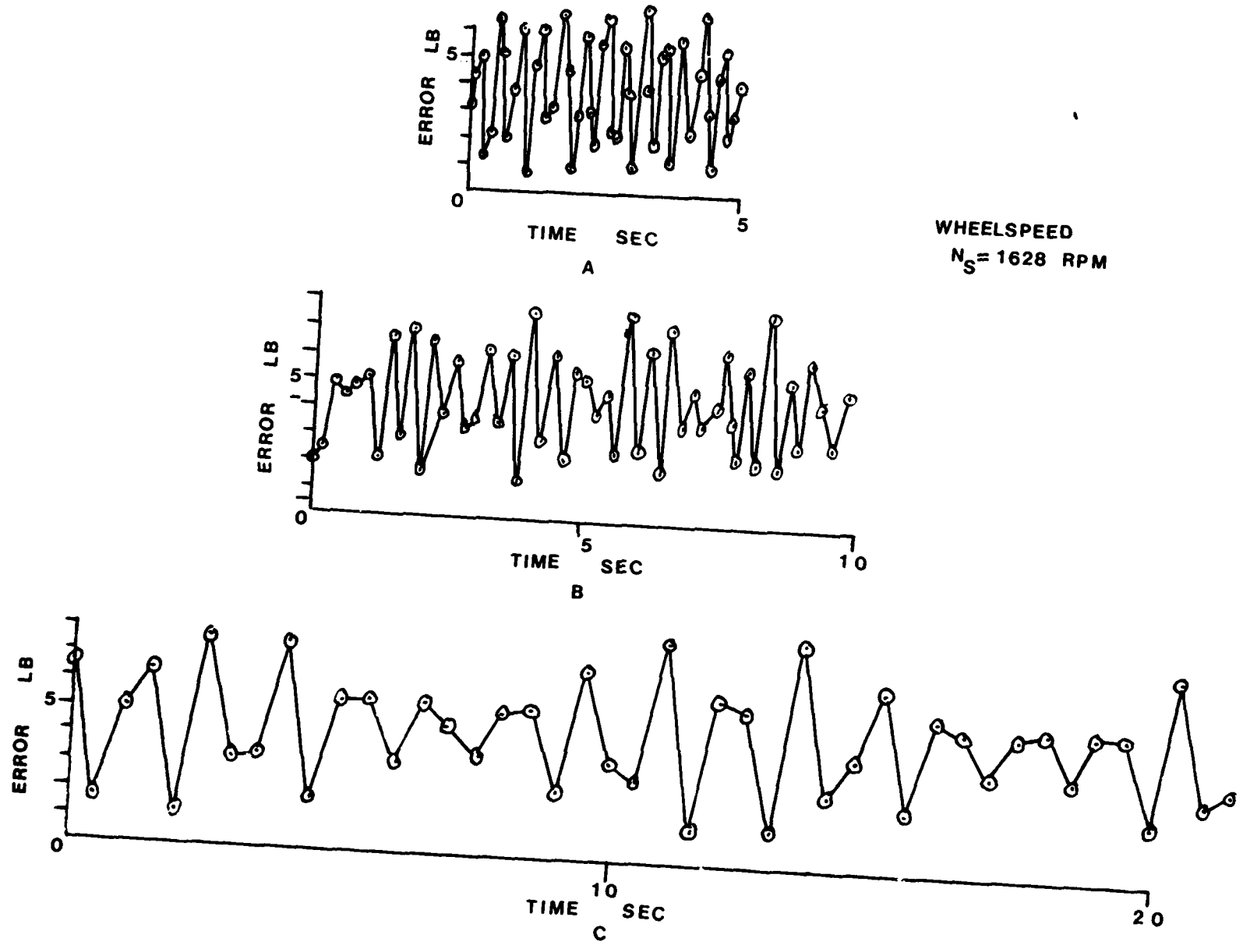
ERROR LB
5
0
TIME SEC
5
A
WHEELSPEED
N_S= 1628 RPM
ERROR LB
5
0
5
TIME SEC
10
B
ERROR LB
5
0
10
TIME SEC
20
C

FIG 37

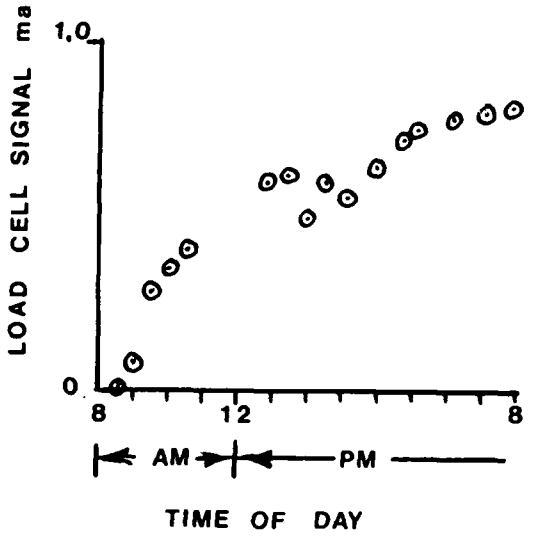

FIG 38

The noise level for this wheelhead is around 6 to 8 lbs. which corresponds to a spindle runout of approximately 20 to 23 microinches. This wheelhead, when used in a grinding machine with 100,000 lb/in. system stiffness, would be capable of holding size to 8 lb/100,000 lb/in. (80 microinches) on radius or 160 microinches on diameter.

From Figures 36a and c, the error signal is seen to have a dominant periodic component of about 13 cy/sec. This wheelhead is built with three pairs of bearings. The front pair have a bore of 110 mm and a retainer speed (the complement of balls) which rotates at .45 times the spindle speed. When running at 1750 rpm the retainer will then be rotating at 13.125 rps. Therefore, the periodic component in Figure 36a and Figure 36c is due to the retainer rotation, and is caused by several balls being about 10 to 12 microinches larger than their neighbors. The load cell "noise" could be reduced by carefully selecting balls of equal size in the front bearing.

Figure 37 shows similar plots of the load cell noise but at a wheelspeed of 1628 rpm. In these tests periodic components close to the spindle speed can be recognized in Figures 37a and 37b, along with a "beat frequency" of about 4.6 cps. Some of the other pairs of bearings in the head may be the cause of the "beat frequency".

Drift tests were also conducted on the load cell wheelhead. The analog output from the load cell was observed over a 12-hour period, first with the wheelhead at rest, and then with the wheelhead running at 1750 rpm. The first test showed no drift whatsoever in the electronics. The second test showed considerable drift as plotted in Fig. 38. Evidently, in this wheelhead as the temperatures increase, an internal misalignment takes place between the three pairs of bearings; i.e., the front bearings, the pair in the middle of the spindle, and the rear bearings at the pulley end. This requires frequent nulling of the load cell. Steps are being taken to do this automatically in the computer.

7.0 Conclusion

From the work presented above it can be concluded that:

1. Significant cost savings can be achieved by CNC multioperation grinding.

2. Force-Adaptive Grinding, using force sensors, provides better control over the grinding process variables; namely, wheelsharpness and induced force thereby reducing the degree of operator attention required, and improving product quality.

3. Elimination of thermal expansion sizing errors can be achieved by either locating the dresser at an invariant distance from the work centerline, or by monitoring the distance and compensating for variations in dresser location by computer to provide drift-free sizing.

4. In form grinding of profiles significant reductions in Grind Time can be achieved with greatly reduced wheelwear by using Creep-Feed Grinding.

5. Force-Adaptive Grinding allows the computer to compensate for deflections in the system to provide greater accuracy.

6. Force-Adaptive Grinding permits the computer to estimate wheelwear and to compensate in sizing for wheelwear as well as to initiate dressing operations to prevent form errors.

7. Force-Adaptive Grinding provides the computer with the ability to monitor the wheel sharpness and to initiate dressing operations to prevent thermal damage of the workpiece.

8. Force sensors can be built into existing wheelheads to provide a reliable load cell capable of operation in harsh production environments.

8.0 Recommendations

It is recommended that:

1. A rotary table creep-feed grinder be obtained and modified to provide a constant temperature reference plate and dressers located relative to the work centerline.

2. A Creep-Feed Force Adaptive-Control be developed for monitoring induced forces, wheel sharpness, compensating for deflections, estimating wheelwear, to provide automatic sizing and form control.

3. Grinding tests be conducted to determine actual cutting stiffnesses, threshold forces, machine stiffness, wheelwear parameters, optimum table speed, ability to compensate for deflections, ability to estimate differential wheelwear and maintain form, ability to monitor wheelsharpness and prevent thermal damage and general ability to produce high quality parts without operator attention.

9.0 Bibliography

1. R. S. Hahn: "The Effect of Wheelwork Conformity in Precision Grinding". Trans. ASME vol 77 no. 8, pp 1325-1329 November 1955

2. R. S. Hahn: "On the Nature of the Grinding Process", Proceedings of the Third MTDR Conf. (1961) pp 129-154, Pergamon Press.

3. R. S. Hahn, R. P. Lindsay: "Principles of Grinding", Machinery, July, August, September, October, November 1971.

4. R. P. Lindsay: "Variables Affecting Metal Removal and Specific Horsepower in Precision Grinding"; SME Paper No. MR71-269.

5. R. P. Lindsay: "On Metal Removal and Wheel Removal Parameters, Surface Finish, Geometry and Thermal Damage in Precision Grinding"; PhD Dissertation, Worcester, MA Polytechnic Institute 1971.

6. R. S. Hahn, R. P. Lindsay: "The Production of Fine Surfaces while Maintaining Good Surface Integrity at High Production Rates by Grinding"; Proc. International Conf. on Surface Technology 1973, SME, Dearborn, MI.

7. G. R. Shafto, A. T. Notter: "Use of CBN Grinding Wheels in High Stock Removal Grinding"; Univ. of Bristol, England, International Conf. on Creep-Feed Grinding, 26, 27 Sept. 1979 pp 137-166.

8. J. Pratt: "The Development of a Small Creep-Feed Surface Grinder"; International Conf. on Creep-Feed Grinding, Univ. of Bristol, England, 26- 27 Sept. 1979, pp 79-92.

9. R. Stauffer: "Creep-Feed Grinding Cuts Cycle Time 60%"; American Machinist, vol. 86 No. 6. June 1981, pp 68-70.

10. E. Salje, H. H. Damlos, H. Teiwes: "Problems in Profile Grinding--Angular Plunge Grinding and Surface Grinding"; Annals of C.I.R.P. vol 30, 1/1981, Hallwag Ltd. Berne.

11. John Taylor: "Metal Bonded CBN, How and Why it Works"; Wickman Corp. Presented at SME International Engineering Conf., Philadelphia, May 17-20, 1982

12. R. S. Hahn: "High Performance Production Grinding Systems"; SME Paper No. MR82-230 (1982).

13. R. S. Hahn: "Computer Control for Small-Hole Grinding"; National Science Foundation Report MEA 8113282, 1982.

10. Professional Personnel

10.1 Biographical Notes of Robert S. Hahn

Robert S. Hahn was employed for nearly 40 years by the Heald Division of Cincinnati Milacron Corp. Since 1944 he has devoted himself to the research and development of machine tools and precision machining processes, serving as Research Engineer, Chief Research Engineer, and Manager of Research for Cincinnati Milacron-Heald Corp. He holds M.E., MSc, and D.Sc. degrees from the University of Cincinnati. He has been a teacher of graduate courses in Vibration, Elasticity, Lubrication Theory at Worcester Polytechnic Institute, and was an Adjunct Professor of Mechanical Engineering at the University of Cincinnati.

Currently he heads the firm Hahn Associates, consulting engineers, offering computer-integrated grinding systems, machine tool R&D and manufacturing process development.

He has spoken at professional convocations throughout the world, and is published in several languages. His many technical papers, books and articles in professional journals have dealt with such subjects as vibration and chatter in precision grinding operations, the relation between grinding conditions and thermal damage in the workpiece, the nature of the grinding process, controlled-force grinding, grinding surface finish, the selection and design of grinding cycles and factors in grinding high-strength, heat-resistant alloys.

He is a registered professional engineer in Massachusetts, a member of the A.S.M.E., the SME, and the American Association for Advancement of Science. He has served on the Executive Committee of the Production Engineering Div. of A.S.M.E., and was chairman of the Division in 1960. He also served as chairman, vice-chairman and secretary of the Worcester Section of A.S.M.E., chairman of the ASME Production Engineering Research Committee, chairman SME Abrasive Cutting Processes Subdivision, and a member of the NMTBA Research and Development Committee. He is also a member of the C.I.R.P. (College International pour letude Scientifique des Techniques de Production Mecanique), a member of Tau Beta Pi, Sigma Xi, and Pi Tau Sigma.

Numerous patents have been issued to him. He was awarded "Master Design Award, sponsored by Product Engineering magazine for his invention of the Controlled-Force Grinding Machine. In 1965 he received the ASME Blackall Machine Tool Award; in 1966 the Scientific Achievement Award presented by the Worcester Engineering Society, the SME Research Medal, and the 1981 ASME Medal for over 40 years of inventions and outstanding contributions to manufacturing, research, in particular to grinding and chatter in precision machining operations.

PUBLICATIONS

R. S. Hahn

1. Design of Lanchester Damper for Elimination of Metal-Cutting Chatter.

   Trans. ASME 1951 V73 pp 331-335

2. Section on Metal-Cutting Chatter in ASTE Handbook

3. Some Observations on Chip Curl in the Metal-Cutting Process under Orthogonal Cutting Conditions.

   Trans. ASME 1953 V75 pp 581-590

4. On the Temperature Developed at the Shear Plane in the Metal-Cutting Process.

   Proc. 1st National Congress of Applied Mechanics published by ASME pp 661-666

5. Advances in Precision Boring

   ASTE Paper No. 21T2-1 1953

6. Metal-Cutting Chatter and Its Elimination

   Trans. ASME 1953 V75 N6

7. On the Theory of Regenerative Chatter in Precision Grinding Operations

   Trans. ASME May 1954 V76 N4 pp 593-597

8. The Effect of Wheelwork Conformity in Precision Grinding

   Trans. ASME Nov. 1955 V77 N8 pp 1325-1329

9. The Relation Between Grinding Conditions and Thermal Damage in the Workpiece

   Trans. ASME May 1956 pp 807-812

10. Vibrations of Flexible Precision Grinding Spindles

    Trans. ASME Series B 1959 N81 pp 201-206

11. Chapter on Self-Excited Vibrations in Shock and Vibration Handbook

    McGraw-Hill 1961

PUBLICATIONS (contd.)

R. S. Hahn

12. On the Analysis of Random Errors in Precision Grinding Operations

    Trans. ASME V83 N2 Series B
    J. Eng. for Industry 1961 pp 131-141

13. On the Nature of the Grinding Process

    Proc. 3rd International Conference on Machine Tool Design and Research
    Birmingham Sept. 1962 Pergamon Press

14. Le broutement en rectification et imperfections des surfaces rectifiees

    No. 1 Jan-Feb. 1963 pp 3-10
    Groupement pour l'avancement de la Mecanique Industrielle
    Revue Bimestrielle 4 et 6 rue
    Gambetta Saint-Ouen (Seine) PARIS

15. Controlled Force Grinding - A New Technique for Precision Internal Grinding

    Trans. ASME J. of Eng. for Ind.
    Series B V68 1964 pp 287-293

16. On the Mechanics of the Grinding Process Under Plunge Cut Conditions

    ASME Paper No. 65 Prod - 7

17. Gyroscopically Induced Vibrations in Grinding Spindles

    Annals of the CIRP Vol. X111 pp 381-388
    Pergamon Press Oxford 1966

18. Some Characteristics of Controlled Force Grinding

    Proc. 6th International Machine Tool Design and Research Conference, Manchester College of Science & Technology
    Pergamon Press Oxford 1966

R. S. Hahn
P. Fleischer
R. C. Griffith 19. On the Selection and Design of Grinding Cycles

Proc. 7th International MTDR Conference
Univ. of Birmingham 1966
Pergamon Press Oxford 1967

R. S. Hahn
R. Lindsay 20. On the Effects of Real Area of Contact and Normal Stress in Grinding

Presented at CIRP Meeting Paris 1966
in Print

R. S. Hahn 21. Some Advantages of Hydrostatics in Machine Tools

ASLE Paper No. 64AM3C1 1964

R. S. Hahn
R. Lindsay 22. Some Factors Affecting Surface Finish in Grinding

Annals CIRP VXIV pp 47-52 Pergamon 1966

R. S. Hahn 23. Vibration Research: The production payoff is here.

Machinery Jan. 1967 67-70

R. S. Hahn 24. Survey of the Technical Factors in Grinding High-Strength, Heat-Resistant Alloys

Annals CIRP VXVII pp 16/1-16/10 Pergamon 1969

R. S. Hahn 25. Vibration Problems and Solutions in Grinding

SME Tech. Paper MR69 - 246

R. S. Hahn 26. The Influence of Process Variables on Material Removal, Surface Integrity, Surface Finish and Vibration in Grinding.

Proc. 10th International MTDR Conf. pp 95-117
Pergamon Press 1970

R. S. Hahn
R. Lindsay 27. Grinding Aerospace Materials

Mecanique No. 252 Dec. 1970 GAMI Paris

PUBLICATIONS (contd.)

R. S. Hahn
R. Lindsay

28. Variables Affecting Metal Removal and Specific Power in Precision Grinding.

Annals of CIRP V 20/1 1971

R. S. Hahn
R. Lindsay

29. The Principles of Grinding

SME Tech. Paper MRR71-01

R. S. Hahn
R. Lindsay

30. On the Basic Relationship between Grinding Parameters

Annals CIRP Vol. XVIV pp 657-666 Pergamon 1971

R. S. Hahn
R. Lindsay

31. The Principles of Grinding

Nat. Bur. Stds Special Publication 348 1972

R. S. Hahn
R. Lindsay

32. On the Rounding-Up Process in High Production Internal Grinding Machines by Digital Computer Simulation

Proc. 12th International Mach. Tool Design and Research Conf.
MacMillan Press Ltd pp 235-240 1972

R. S. Hahn
R. Lindsay

33. The Relationship between Wheel Characteristics and Operating Problems in High Production Precision Grinding

Proc. 13th Int. Mach. Tool Design & Research Conf. 1973

R. S. Hahn
R. P. Lindsay

34. Factors Affecting Precision in High Production Internal Grinding

SME Manufacturing Engineering Trans. Vol 2 1973

R. S. Hahn
R. Lindsay

35. The Production of Fine Surface Finishes while Maintaining Good Surface Integrity at High Production Rates by Grinding

14th International MTDR Conf.
MacMillan Press Ltd 1974

R. S. Hahn 36. Grinding Software - An Important Factor in Reducing Grinding Costs

Proc. International Conf. on Prod. Eng'g Tokyo, Japan, Soc. Prec. Eng. 1974

R. S. Hahn 37. Reducing Grinding Costs Through Improved Grinding Technology

SME Tech. Paper MR75-603 1975

R. S. Hahn 38. Neue Entwicklung beim Genauschleifen

wt-Z. ind. Fertig. 65 453-461 Springer Verlag 1975

R. S. Hahn 39. On the Loss of Surface Integrity and Surface Form due to Thermoplastic Stress in Plunge Grinding Operations

Annals CIRP V 25/1/1976 pp. 203-208

R. S. Hahn 40. The Fundamentals of Precision Grinding

SME Technical Paper MR76 -370 1976

R. S. Hahn 41. The Influence of Grinding Machinability Parameters on the Selection and Performance of Precision Grinding Cycles.

Proc. Int. Conf. Machinability Testing and Utilization of Data

ASM Sept. 1978

R. S. Hahn 42. Grinding Chatter in Precision Grinding Operations - Causes and Cures

SME Tech. Paper MR78-331 1978

R. S. Hahn 43. The Influence of Threshold Forces on Size, Roundness and Contour Errors in Precision Grinding.

Annals of CIRP vol 30/1/1981, Hallwag Ltd.Berne

R. S. Hahn 44. High Performance Grinding Systems

SME Paper No. MR82-230

R. S. Hahn 45. Precision Grinding Bodies of Revolution--An Alternative to Diamond Turning.

SME Paper No. MR82-928

U. S. PATENTS

3,269,063	3,492,894
2,651,223	3,555,741
2,699,696	3,582,525
2,680,941	3,601,931
2,647,348	3,605,344
3,089,288	3,634,976
3,056,238	3,644,049
2,930,167	3,640,138
2,881,568	3,642,378
2,873,121	3,694,969
3,197,921	3,554,062
3,547,795	3,499,350
3,540,269	3,745,710
3,387,899	3,874,809
3,431,685	3,913,277
	4,008,631

10.2 Biographical Notes of Douglas A. Wiles

Education:

1970-1974 Rensselaer Polytechnic Institute, Troy, New York, B. S. Electrical Engineering.

Employment History:

1979-present

GenRad, Inc., Concord, Massachusetts, Senior Development Engineer in area of Automatic Test Equipment specification and development.

System engineering department; responsible for overseeing design of new automatic test equipment (GenRad's major product line). Duties include producing product descriptions and design specification and providing interdisciplinary coordination during design and implementation phases of new product development.

Product business group; participated in determination and definition of improvements to existing products and direction for new product goals.

Software engineering; lead software engineer in charge of team to design and implement software for functional test systems. Specialties included simulation of printed circuit board logic and modeling of LSI.

Presentations; "Functional Modeling of LSI for Simulation", Nepcon West, February 1980.

"Future Trends in Functional Testing", ATE show, Boston, MA June 1980.

1975-1979

Westinghouse Electric Corp., Baltimore, Maryland, Engineer in area of military systems.

Software design; lead software engineer for development and maintenance of software on the Air Force electronic counter measure ALQ-131 project. Duties included determination of requirements, specification and production of necessary software, support of flight test and creation of documentation to military standards.

1974-1975

Sperry Univac, Utica, New York, Engineer in Quality Assurance.

Design engineer; responsible for electronic and and software design and implementation of numerical control system based on 8080 microprocessor.

10.2 Biographical Notes of Douglas A. Wiles--contd.

Personal Facts:

U. S. Citizen
Birth date: February 23, 1952
Married
Member IEEE
President of college fraternity alumni organization

11.0 Interactions

There are no plans at this time to present this material in a technical paper. However, some presentations may be made in the future.

The principle investigator serves as a seminar leader for American Machinist, and may discuss certain aspects of this work in these technical seminars.

12.0 Inventions

The method proposed in this report for referencing two independent cross-slides to a common isothermal reference related to the work centerline may be a novel approach to holding size automatically on large grinding machines. The computerized acquisition of wheelwear data by the introduction of a Wheelwear Measurement Station and the use of this data to estimate and compensate for wheelwear during grinding operations may also be a novel solution.

TABLE 1 TURBINE VANE SEGMENT PROCESSING TIME

CNC MULTIOPERATION	Time/hr.	CURRENT METHOD	Time/hr.
SETUP NO. 1		SET UP BRYANT INTERNAL	
Oper. 320,330		Oper. 320	2.08
Part of 354,350	.30	Oper. 330	.585
SETUP NO. 2		SET UP SHEFFIELD EXTERNAL	
Oper. 352,354	.183	Oper. 340	.585
SETUP NO. 3		SET UP 36" BULLARD	
Oper. 420,430,340	.48	Oper. 350	2.60
		SET UP BRYANT INTERNAL	
		Oper. 352	
		Oper. 354 (Both)	2.18
		SET UP SHEFFIELD INTERNAL	
		Oper. 420	.73
		Oper. 430	.61
TOTAL MACHINING TIME	.963	TOTAL MACHINING TIME	9.37

TABLE 2 ESTIMATED GRIND TIMES - SET UP NO. 1

OPER. 1: VECTOR GRIND NO. 1 HEAD
(Oper. 320,330, Part of 350)

INDEX TO WORKPIECE	10 sec.
VECTOR FEED .050 in. @ .0002 in/sec.	295*
DRESS	25
VECTOR FINISH .010 in. @ .0002 in/sec.	50
RETRACT	10

OPER. 2: VECTOR GRIND NO. 2 HEAD
(Oper. 350, Part of 352 & 354)

INDEX TO WORKPIECE	10
VECTOR FEED .050 in. @ .0002 in/sec.	295
DRESS	25
VECTOR FINISH .010 in. @ .0002 in/sec.	50
RETRACT	10
UNLOAD AND LOAD	300
Floor-To-Floor Time	1080 sec.
	0.3 hr.

*INCLUDES 45 SEC. SPARKOUT TIME

TABLE 3 ESTIMATED GRIND TIMES - SET UP 2

OPER. 1: 12^{o} VECTOR GRIND BOTH HEADS SIMULTANEOUSLY (OPER. 352,354)

INDEX TO WORKPIECE.....	10 sec.
VECTOR FEED .020 in. @.00016 in/sec.	125
DRESS	25
VECTOR FEED .020 in. @.00016 in/sec.	125
DRESS	25
VECTOR FINISH .005 in. @.00016 in/sec. ..	30
RETRACT	10
UNLOAD AND LOAD	300
Floor-To-Floor Time	650 sec.
	0.183 hr.

TABLE 4 ESTIMATED GRIND TIMES - SET UP 3

OPER. 1: VECTOR GRIND NO. 1 HEAD
(Oper. 430)

INDEX TO WORKPIECE	10
VECTOR FEED .050 in. @.0002 in/sec.	295
DRESS	25
VECTOR FINISH .010 in. @.0002 in/sec.	50
RETRACT	10

OPER. 2: VECTOR GRIND NO. 1 HEAD
(Oper. 420)

INDEX TO WORKPIECE	10
VECTOR FEED .050 in. @.0002 in/sec.	295
DRESS	25
VECTOR FINISH .010 in. @.0002 in/sec.	50
RETRACT	10

OPER. 3: X GRIND OD NO. 2 HEAD
(Oper. 340)

INDEX TO WORKPIECE	10
X FEED .050 in. @.00009 in/sec.	555
DRESS	25
X FINISH .005 in. @.00017 in/sec.	30
RETRACT	10
UNLOAD AND LOAD	300
Floor-To-Floor Time	1710 sec.
	.475 hr.

TABLE 5 VANE-CLUSTER ASSEMBLY PROCESSING TIME

CNC MULTIOPERATION

SET UP GRINDER

L.H.	Grind Oper. 40 and Part of Oper 50 .255in. @.008	-
R.H.	Grind Oper. 50 (ID) and Oper. 60 .390in. @.006	65.min.
	Index RH to Oper.70	.1
	Grind Oper.70 (18 Parts) .040in. @.0015	26.7
	Unload & Load	10.0
	Floor-to-Floor Time	101.8min.

18 Parts Complete

CURRENT METHOD

SETUP 52 IN BULLARD GRINDER
Left Head Only

Grind Oper. 40 (18 Parts)	
L.H. OD .255in.@.008in/min	31.9m
Unload and Load	10.0

SETUP 52 IN BULLARD GRINDER
Both Heads

Grind Oper. 50 (18 Parts)	
L.H. OD .160 @.008in/min	-
R.H. ID .290 @.008in/min	36.25
Unload and Load	10.0

SETUP 52 IN BULLARD GRINDER
Both Heads

Grind Oper. 60 (18 Parts)	
L.H. ID Rough Groove .290 @.006	-
R.H. ID Finish Groove .390 @.006	65.00
Unload and Load	10.0

SET UP B&S SURFACE GRINDER

Grind Oper. 70 (4 Parts)	
.040 in. @ .0015	26.7
Unload and Load	3.0

Floor-to-Floor Time for 18 Parts:

41.9+46.25+75.+4.5 (29.7) = 296.8mi

TABLE 6: SOME TYPICAL VALUES OF CREEP FEED GRINDING PARAMETERS

h mm	V_w $\frac{mm}{min}$	V_s $\frac{m}{s}$	P' $\frac{w}{mm}$	Λ_{w_3} $\frac{mm^3}{min \cdot N}$	D_e m	REF.	COMMENTS
7.6	330	30	315	118.	1400.	9	Wheel: Al_2O_3 Mat'l: 15B35 Carbon Steel Induction Hard'nd R_c 30-40
1.25	304	20	-	-	260.	11	Wheel: Metal Bonded CBN Mat'l: M2 R_c 62-64
2.0	100	50	-	11.6	3750.	7	Wheel: ABN360 DeBeers Resin Bonded Mat'l: M2
5.0	100	50	-	14.5	3750.	7	Wheel: ABN300 DeBeers Electroplated Mat'l: M2
1 to 4	30 to 100	30	-	5 to 60	16000. 1600.	8	Wheel: Al_2O_3 Mat'l: K9 Oil Hardened Cast Tool Steel

TABLE 6

TABLE 7--WHEELWEAR THICKNESS Z'_s/V_s vs PRESSURE
CONTROLLED FORCE INTERNAL GRINDING

Wheelspeed	12500 sfm
Workspeed	465 sfm
Work Diameter	3.62 inch
Wheel Diameter	3.25 inch
Coolant	Florex
Work Material	AISIE 52100 @ R_c 60
Dress Lead	0.004 inch/rev.

	Dress Ratio	Wheel
○ ●	0.25, 0.50	12A80K8VFMD2
□ ■	0.25, 0.50	12A80P8VFMD2
△ ▲	0.25, 0.50	2A80K4VFMD2
▽ ▼	0.25, 0.50	2A80P4VFMD2

TABLE 8--WHEELWEAR THICKNESS Z'_s/V_s vs PRESSURE
CONTROLLED FORCE ROTARY SURFACE GRINDING

Wheelspeed	11500 sfm
Workspeed	465 sfm
Work Diameter	3. inch O.D. x 2 inch I.D.
Wheel Diameter	3.25 inch
Dress Lead	0.004 inch/rev.
Dress Ratio	0.25
Work Material	AISIE 52100 @ R_c 60
○ ◐ ● Wheel	32A60M8VBE
□ ◧ ■	12A80P4, 2A80P4 and 12A80K4VFMD2 respectively

For Rene 80 @ R_c 30-32

△ Wheel	32A60M8VBE
▼	32A70K8VBE with:
Workspeed	500 sfm
Dress Lead	0.004 inch/rev.

TABLE 8--continued

Dress Ratio	0.25
Wheelspeed	11500 sfm
Workspeed	Various
Coolant	Florex @ 200 psi
Wheel Diameter	3.25 inch
Work Diameter	3 inch O.D. x 2 inch I.D.

Symbol	Wheel	Wheelspeed	Lead	c/ℓ
●	32A60M8VFM	11000 sfm	0.004	0.25
▲	32A70K8VFM	11000 sfm	0.004	0.25
▼	32A60M8VFM	11000 sfm	0.001	0.50
■	32A70K8VFM	5000 sfm	0.001	0.50

TABLE 9--WHEELWEAR THICKNESS Z'_s/V_s vs PRESSURE
CONTROLLED-FORCE EXTERNAL GRINDING

Symbol	Wheel	Dress Ratio
⊙	12A80K4VFMD2	0.25
●	12A80K4VFMD2	0.50
□	12A80P4VFMD2	0.25
■	12A80P4VFMD2	0.50
△	2A80K4VFMD2	0.25
▲	2A80K4VFMD2	0.50
▽	2A80P4VFMD2	0.25
▼	2A80P4VFMD2	0.50

Wheelspeed	12500 sfm
Workspeed	465 sfm
Wheel Diameter	3.25 inch
Work Diameter	5.25 inch
Dress Lead	0.004 inch/rev.
Coolant	Florex @ 200 psi
Work Material	AISIE 52100 @ R_c 60


ME